Journal Pre-proofs

A review on the latest developments of mesoporous silica nanoparticles as a promising platform for diagnosis and treatment of cancer

Fatemeh Ahmadi, Arezoo Sodagar-Taleghani, Pedram Ebrahimnejad, Seyyed Pouya Hadipour Moghaddam, Farzam Ebrahimnejad, Kofi Asare-Addo, Ali Nokhodchi

PII: S0378-5173(22)00653-6
DOI: https://doi.org/10.1016/j.ijpharm.2022.122099
Reference: IJP 122099

To appear in: *International Journal of Pharmaceutics*

Received Date: 22 March 2022
Revised Date: 24 July 2022
Accepted Date: 5 August 2022

Please cite this article as: F. Ahmadi, A. Sodagar-Taleghani, P. Ebrahimnejad, S. Pouya Hadipour Moghaddam, F. Ebrahimnejad, K. Asare-Addo, A. Nokhodchi, A review on the latest developments of mesoporous silica nanoparticles as a promising platform for diagnosis and treatment of cancer, *International Journal of Pharmaceutics* (2022), doi: https://doi.org/10.1016/j.ijpharm.2022.122099

A review on the latest developments of mesoporous silica nanoparticles as a

Fatemeh Ahmadi[1,†], Arezoo Sodagar-Taleghani[2,3,†], Pedram Ebrahimnejad[1,4,†,*], Seyyed Pouya Hadipour Moghaddam[5,6], Farzam Ebrahimnejad[7], Kofi Asare-Addo[8], Ali Nokhodchi[9*]

[1]Department of Pharmaceutics, Faculty of Pharmacy, Mazandaran University of Medical Sciences, Sari, Iran; [2]Department of Petroleum and Chemical Engineering, Science and Research Branch, Islamic Azad University, Tehran, Iran; [3]Young Researchers and Elite Club, Science and Research Branch, Islamic Azad University, Tehran, Iran; [4]Pharmaceutical Science Research Center, Hemoglobinopathy Institute, Mazandaran University of Medical Sciences, Sari, Iran; [5]Utah Center for Nanomedicine, Nano Institute of Utah, University of Utah, Salt Lake City, UT 84112, USA; [6]Electrical and Computer Engineering, University of Utah, Salt Lake City, UT 84112, USA; [7]Paul G. Allen School of Computer Science and Engineering, University of Washington, Seattle, USA; [8]Department of Pharmacy, School of Applied Sciences, University of Huddersfield, Huddersfield, UK; [9]Pharmaceutics Research Laboratory, School of Life Sciences, University of Sussex, Brighton, UK

†Contributed equally as first authors.

***Corresponding Authors:**
Pedram Ebrahimnejad (pebrahimnejad@mazums.ac.ir)
Ali Nokhodchi (a.nokhodchi@sussex.ac.uk)

Abbreviation	Explanation
MSNs	Mesoporous silica nanoparticles
DDS	Drug delivery system
SBA	Santa Barbara Amorphous
MCM	Mobile Crystalline Material
MSU	Michigan State University Materials
PAA	Poly acrylic acid
CTAB	Cetyltrimethylammonium bromide
EPR	Enhanced permeability and retention
MDR	Multidrug resistance
HeLa	Human cervical carcinoma
DOX	Doxorubicin
β-CD	β-cyclodextrin
PEG	Polyethylene glycol
HMSNs	Hollow mesoporous silica NPs
VEGF	Vascular endothelial growth factor
PDA	Polydopamine
HA	Hyaluronic acid
PDT	Photodynamic therapy
SCC7	Squamous cell carcinoma 7
ETS	Etoposide
PEMs	Polyelectrolyte multilayers
GSH	Glutathione
DTT	Dithiothreitol
Cyt C	Cytochrome C
TPT	Topotecan
US	Ultrasonic
NIR	Near-infrared
CuS	Copper sulfide
MRI	Magnetic resonance imaging
OI	Optical imaging
PET	Positron emission tomography
CT	Computed tomography
PNIPAAM	Poly(N-isopropyl acrylamide)
LCST	Low critical solution temperature
PEI	Poly(ethylenimine)
HER2	Human epithelial growth factor receptor 2
GQDs	Graphene quantum dots

CDs	Carbon dots
RES	Reticuloendothelial system
TPGS	Tocopheryl polyethylene glycol 1000 succinate
PLH	Poly (L-histidine)
TAT	Trans-Activator of Transcription
MPS	Mononuclear Phagocyte System

Abstract

Cancer is the second cause of human mortality after cardiovascular disease around the globe. Conventional cancer therapies are chemotherapy, radiation, and surgery. In fact, due to the lack of absolute specificity and high drug concentrations, early recognition and treatment of cancer with conventional approaches have become challenging issues in the world. To mitigate against the limitations of conventional cancer chemotherapy, nanomaterials have been developed. Nanomaterials exhibit particular properties that can overcome the drawbacks of conventional therapies such as lack of specificity, high drug concentrations, and adverse drug reactions. Among nanocarriers, mesoporous silica nanoparticles (MSNs) have gained increasing attention due to their well-defined pore size and structure, high surface area, good biocompatibility and biodegradability, ease of surface modification, and stable aqueous dispersions. This review highlights the current progress with the use of MSNs for the delivery of chemotherapeutic agents for the diagnosis and treatment of cancer. Various stimuli-responsive gatekeepers, which endow the MSNs with on-demand drug delivery, surface modification strategies for targeting purposes, and multifunctional MSNs utilized in drug delivery systems (DDSs) are also addressed. Also, the capability of MSNs as flexible imaging platforms is considered. In addition, physicochemical attributes of MSNs and their effects on cancer therapy with a particular focus on recent studies is emphasized. Moreover, major challenges to the use of MSNs for cancer therapy, biosafety and cytotoxicity aspects of MSNs are discussed.

Keywords: Mesoporous silica; Nanoparticles; Cancer therapy; Diagnostics; Drug delivery

1. Introduction

Cancer is a combination of a large group of diseases with several environmental and genetic factors. Common genetic and external factors that impact cancer death in humans include exposure to physical carcinogens, chemical carcinogens, environmental pollutants, diet and obesity, infections, biological carcinogens, and radiation. Conventional methods for the treatment of cancer include chemotherapy, radiotherapy, and surgery (Hasan-Nasab et al., 2021; Mohammady et al., 2016). Unfortunately, radiotherapy and surgery are limited to the treatment of localized cancers that are found in one area of the body (Baskar et al., 2012). On the other hand, although chemotherapy is a treatment for advanced cancers that enter the bloodstream or lymph system, most anticancer drugs cause severe side effects on healthy cells and are limited by cancer cells induced multidrug resistance (MDR) (Bukowski et al., 2020; Kankala et al., 2020b). It is therefore vital to develop new strategies for the targeted delivery of chemotherapeutics to release them precisely at the tumor site and thereby reducing side effects, MDR, metastasis, and tumor recurrence caused by traditional treatments (Sodagar-Taleghani et al., 2021). For diagnosis, monitoring, and treatment of cancer, nanotechnology can be a promising strategy for the development of drug delivery systems (DDSs) (Sodagar-Taleghani et al., 2020).

So far, the differences in nanoscale DDSs have been greatly observed in increasing the effectiveness of anticancer agents. The highest therapeutic efficiency for delivery into anticancer DDS has been obtained for average particle diameters lower than 100 nm. At a scale of 1-100 nm, nanomaterials have a large surface area and high functional groups on their surfaces, which allow them to be conjugated with several diagnostic and therapeutic agents. Nanoparticles (NPs) represent a wide range of substances that effectively improve drug delivery via conquering

anatomical and chemical barriers within the cancer microenvironment. This enhances the mean circulation time by reducing renal clearance and increasing active targeting (Yao et al., 2020)

The high capacity of nanomaterials for the loading of therapeutic agents is considered a novel approach for achieving considerable therapeutic efficacy with minimal side effects, especially for cancer medicines. Generally, a high specific surface area is one of the main advantages of all nanomaterials (Sadeghi-Ghadi et al., 2021). Nanomaterials have received much attention as they can be utilized in different fields based on their unique electrical, optical, biological, magnetic, mechanical, thermal, and catalytic properties. When a specific surface area per mass of a material increases, a greater amount of nanomaterials can come into contact with microorganisms, which can affect reactivity. The characteristics of the nanostructures such as chemical modification, or coating, size distribution and, surface morphology/topography can influence the anticancer properties of drugs (Raj et al., 2021; Sadeghi-Ghadi et al., 2020). Although a large number of nanomaterials with various morphologies have been synthesized, some NPs have been extensively used in medical and anti-tumoral fields. NPs possess unique physical and chemical properties that allow the prediction of their interaction in both prokaryotic and eukaryotic cells (Rosenblum et al., 2018).

NPs in the field of biomedicine (sensing, drug delivery, photo-thermal therapy, imaging, etc.), can be used as probes to study biological processes. NPs can be arranged into various groups based on their size, shape, morphology, and physical and chemical properties. Some include different carbon group-based NPs, ceramic NPs, polymeric NPs, metal NPs, semiconductor NPs, and lipid-based NPs. NPs have two main classifications based on their composition, which include organic and inorganic nanomaterials. These NPs are used to protect drugs from degradation and control the release of drugs, especially drugs conjugated to NPs, resulting in

extended retention/accumulation in the target area. Many organic NPs induce strong anticancer efficacy, but their clinical applications are limited due to the lack of stability (Li et al., 2017b).

Among the various NPs, mesoporous silica nanoparticles (MSNs) have had enormous considerations due to features which include their tunable and uniform pore size, high pore volume, large surface area, ease of surface modification, external and internal pores, the gating function of the pore opening, high biocompatibility and biodegradability, high mechanical and thermal stability, high loading capacity, and stable aqueous dispersions (Gupta et al., 2020; Liu et al., 2021; Narayan et al., 2018). This review provides an overview of the updated achievements in the use of MSNs drug delivery including their characteristics, efficacy, and toxicity as a versatile platform for both diagnosis and therapy of cancer. The review also addresses the challenges and future outlook of MSNs.

2. Mesoporous Silica Nanostructures

MSNs have gained considerable attention as promising platforms for different biomedical applications (Deodhar et al., 2017; Sodagar-Taleghani et al., 2019; Yu et al., 2017) particularly for diagnosis (M Rosenholm et al., 2011), biosensing (Hasanzadeh et al., 2012), targeted drug delivery (Bharti et al., 2015), and cellular uptake mechanisms (Huang et al., 2010). MSNs can enhance drug solubility and stabilize/control different therapeutic agents (Suzukin et al., 2004). Researchers have indicated that MSNs can effectively induce endocytosis *in vitro* with various kinds of mammalian cancer cells including CHO, Panc-1, lung, and HeLa (human cervical carcinoma) (Živojević et al., 2021). The unique structural properties of MSNs make it a suitable reservoir for loading therapeutic/diagnostic agents as has been described as an invention in some patents (Table 1). The hydrophobic core of mesoporous silica is useful for drug loading whereas

the hydrophilic surface blocks opsonic phagocytosis and leads to easier motion in the body (Kankala et al., 2020c).

MSNs can be divided into different families depending on the pore size, particle diameter, surface area, and synthesis method. Among various mesoporous silica structures, Santa Barbara Amorphous (SBA-), Mobile Crystalline Material (MCM-), and Michigan State University Materials (MSU-) families have been widely studied for drug delivery. Figure 1 indicates the commonly used MSNs in the formulation of DDSs (Trzeciak et al., 2021).

Sol-gel method (Singh et al., 2014), flame synthesis (Kammler et al., 2004), and reverse microemulsion (Finnie et al., 2007) are the most common techniques used to synthesize MSNs. The sol-gel technique is widely applied to synthesize silica nanostructures due to its ability to control the morphology, size distribution, and particle size by monitoring the reaction variables (Rahman and Padavettan, 2012). MSNs can be fabricated using tetraethyl orthosilicate (TEOS) as a precursor. Water is the most commonly used solvent for the manufacture of MSNs through the sol-gel process (Lei et al., 2020).

The biological behavior of NPs (*e.g.,* cytotoxicity, biocompatibility, and biodegradability,) is affected by changes in the NP's size, shape, pore, and surface properties. Hence, the setting up of the physicochemical properties has gained much attention to ascertain an appropriate biological function. To achieve MSNs as an ideal carrier in DDS, the size of particles, the shape of particles, and topology are considered to improve loading capacity. These factors can be adjusted by varying the experimental factors including changing the temperature, the reaction mixture pH, type and concentration of surfactant as well as the source of silica. Adjusting the synthesis parameters such as methanol's amount ratio in the solvent causes the size of the mono-dispersed MSNs with radial rowed mesoporous to range from tens to several hundred nanometers

(Rahikkala et al., 2018).

The MSNs with various pore sizes can be tailored by selecting the different types of surfactants

The longer hydrophobic chain in surfactants gives rise to MSNs with high pore sizes whereas the shorter chain length results in MSNs with smaller pores (Egger et al., 2015; Ganguly et al., 2010; Yano and Fukushima, 2004). The origin of the high surface area in MSNs may be attributed to the presence of nanochannels in each silica crystal membrane (Narayan et al., 2018).

To fabricate dual-mesoporous materials, binary surfactants are used. For instance, Niu and coworkers synthesized core-shelled MSNs with bimodal porosities with a larger tunable pore structure in the core and smaller tunable pore in the shell by using an amphiphilic block copolymer composition (polystyrene-b-poly(acrylic acid), PS-b-PAA) and cetyltrimethylammonium bromide (CTAB) as co-templates particles (Niu et al., 2010). Besides ammonia, other organic amines have also been widely used to provide the effect of basicity on the synthesis of MSNs. Bein *et al.* demonstrated that a substitute reaction of the base triethanolamine based on NaOH or NH_4OH was an efficient reaction system for the preparation of colloidal MSNs with diameters of 20-150 nm (Moeller et al., 2007).

3. Therapeutic Applications of MSNs

3.1 Functionalization of MSNs for Active Tumor Targeting

The surface properties of MSNs are usually insufficient in terms of the induction of the desired biological response or inhibiting a potentially adverse reaction. They should therefore be functionalized before application or any further processing such as coating with functional materials. Surface functionalization of MSNs can be used to improve their physical properties to confirm higher drug adsorption, better drug delivery, and in obtaining extended drug release in

target cells (Natarajan and Selvaraj, 2014). Das et al. proved that the functionalization of MSNs with organic groups increases drug absorption. This may be due to the strong hydrogen bonding

interaction between the carboxylic acid groups of some drugs and the amino groups of the amine-modified mesoporous particles (Das et al., 2020).

The incorporation of long-chain organic compounds (-C8 and -C18 groups) onto the MSNs has a certain effect on their properties. There are three main types of the most common modifications for MSNs: reduction of the pore size, chemical interaction among the pore surface and adsorbed pharmaceutical drug, and the reduction of the humidity of the surface area of the pore *via* aqueous solutions (Doadrio et al., 2006).

An important surface property of MSNs is their charges or covalent bonding to a variety of functional groups such as amino, sulfhydryl, and carboxyl groups (Croissant et al., 2018). The different features of various functional groups can produce different interactions with the host drug molecules through favorable interactions such as covalent bonding, electrostatic attraction, or hydrogen bonding (Cheng et al., 2011). MSNs with proper surface modifications can therefore be good candidates for efficient drug loading and in providing effective drug release. MSNs can be functionalized organically by using different approaches such as post-synthesis (grafting) and direct synthesis (co-condensation) methods (Lee et al., 2009). Silanol groups (Si-OH) on the nanopores surface and the outermost surface of MSNs act as an anchor for chemical cross-linking. This unique feature provides MSNs with two distinct domains that can be individually modified. The internal pores can keep DNA, RNA, drugs, and a large number of organic molecules such as fluorescent or magnetic resonance imaging (MRI) contrast agents. The outer surface can be modified to provide site-specific drug targeting capacity for intracellular delivery (Wu et al., 2011).

The main feature of multifunctional MSNs is their ability to selectively deliver anticancer agents to tumor tissues. Here, the toxic side effects on normal cells can be minimized. To achieve this aim, active and passive targeting or a combination of both targeting needs to be developed. Passive targeting of tumors can be achieved by the enhanced permeability and retention (EPR) effect (Bertrand et al., 2014; Mir and Ebrahimnejad, 2014). Solid tumors grow rapidly, and this comes with increased nutrient and oxygen demand in tissues. As a result, new capillary blood vessels are generated, and this process is called angiogenesis. Compared with healthy blood vessels, these new vessels are often disordered, discontinuous and contain several fenestrations. Due to the enhanced permeability of the EPR effect, the NPs can leak into tumor tissues through the gaps. Moreover, owing to the poor lymphatic drainage of solid tumors, molecules smaller than 4 nm can diffuse back to the blood circulation, whereas the diffusion of larger NPs is hindered, thus accumulating in solid tumors. This phenomenon refers to the retention of the EPR effect (Figure 2) (Fox et al., 2009).

Although passive targeting *via* the EPR effect is a good strategy for the delivery of chemotherapeutic agents, it has several drawbacks such as the inability to distinguish between healthy and diseased tissues, inadequate tumor accumulation, inter- and intra-tumor as well as inter-individual tumor heterogeneity (Subhan et al., 2021). Active targeting and second-generation nanomedicines with improved functionalities and increased efficacy have therefore been applied in overcoming the obstacles of passive targeting. This is usually accomplished by the attachment of a targeting ligand on the outer surface of MSNs, which is specific for the corresponding receptor. Using cancer-specific targeting ligands for modification of MSNs surfaces can improve cellular uptake of MSNs into cancerous cells compared to healthy cells (Sodagar-Taleghani et al., 2021). Various types of ligands have been used for targeting purposes,

237 such as peptides, aptamers, small molecules like folate and mannose derivatives, proteins
238 including lectin, lactoferrin, transferrin, DARPins, monoclonal antibodies, and their engineered

239 fragments, which specifically attach to receptors overexpressed at the target area (Jafari et al.,
240 2016; Sharifi et al., 2021a; Srinivasarao and Low, 2017).
241 Folic acid is a vitamin that acts as a targeting ligand and can be conjugated to the therapeutic
242 molecule for targeting folate receptors overexpressed in numerous human cancer cells found in
243 the breast, ovarian, colorectal, endometrial, and lung (Ebrahimnejad et al., 2021). Apart from
244 folic acid, other small cell nutrient molecules such as mannose have been shown to selectively
245 enhance the cellular uptake of MSNs by breast cancer cells. For example, Tamanoi *et al.* showed
246 high efficacy for the delivery of camptothecin as a hydrophobic anticancer drug, with MSNs as a
247 drug delivery carrier (Lu et al., 2007). The experiments showed that cellular uptake efficiency in
248 the cancer cells was improved by attaching folic acid to the MSN surface.
249 Knežević *et al.* constructed folic acid-modified MSNs with pore-bonded vinblastine and
250 fullerenol-capped as an anticancer drug. The efficacy of therapy on the targeting of cancer-
251 overexpressed folate receptors compared to cell viability after the healthy MRC-5, cervical
252 cancer HeLa cells, and breast cancer MCF-7 therapy indicate that the cancer-targeting ability of
253 the DDS and folate receptor-dependent activity of the prepared material may be constructed for
254 tumor tissues selective therapy (Knežević et al., 2016).
255 Carbon dots (CDs) as novel kind of fluorescent carbon-based nanomaterials have attracted great
256 attentions in various research fields such as drug delivery, bioimaging, and biosensors (Wan et
257 al., 2021). Sun and coworkers prepared a fluorescent mesoporous silica-carbon dot nanohybrid.
258 CDs, from folic acid as the raw material, were synthesized *in situ* and functionalized via a
259 microwave-assisted solvothermal reaction on the amino-modified MSNs (MSNs-NH_2) surface.

The nanohybrid showed bright yellow emission-stable and retained the MSNs' superior features showing the ability for fluorescence imaging guided drug delivery. This MSNs-CDs nanohybrid was utilized to target folate receptor-overexpressing HeLa cells. Due to the FA function-alike structure of the CDs on the surface of MSNs, it is considered a nanocarrier for efficiently delivering drugs into tumor environments and subsequently reducing the side effects of chemotherapy (Figure 3) (Zhao et al., 2019).

In another study, iron oxide core@shell MSNs were fabricated and decorated with polyethyleneimine (PEI) layer and folic acid moieties for efficient delivery of erlotinib. The results showed that the folate-targeted NPs had higher toxicity in HeLa cells in comparison with the free erlotinib (Avedian et al., 2018).

Park *et al.* showed cancer cell-targeting NPs which can load multiple therapeutic agents for important therapeutic effects and specific therapies for cancer. To achieve these goals, hyaluronic acid (HA) was attached to targeting MSNs for efficient cancer cell drug delivery. To minimize the side effects of chemotherapy and synergistic therapeutic effects of chemotherapy. CD44-targetable MSNs have been used for chemotherapy and photodynamic therapy (PDT). HA-MSNs are remarkable nanocarriers with favorable CD_{44}-targeting with the ability for efficient delivery of dual-drug (Ce6 and doxorubicin (DOX)) to CD_{44}-expressing squamous cell carcinoma 7 (SCC7) cells. DOX/Ce6/HA-MSNs indicated high efficient cytotoxicity on green fluorescent protein-expressing SCC7 whereas up to 250 µg/ml of HA-MSNs was viable for most of the cells (>95%). This suggested that HA-MSNs are non-toxic and biocompatible nanocarriers (Park et al., 2019).

Wang *et al.* fabricated HB5 aptamer-modified mesoporous silica-carbon-based DOX-loaded nanosystems (MSCN-PEG-HB5/DOX) which were characterized for the treatment of human

283 epithelial growth factor receptor 2 (HER2)-positive breast cancer cells (Wang et al., 2015).
284 Aptamer HB5 modified NPs indicated significantly higher cellular uptake in HER2 positive

285 breast cancer in comparison to the untargeted particles, thereby leading to the highest cell-killing
286 effect.
287
288 **3.2. MSNs-based controlled release systems for cancer treatment**
289 It is necessary to inhibit the initial burst release of drugs from DDSs enabling the nanocarriers to
290 ensure the ability to release drugs at the right place and time. To design and equip MSNs with
291 controlled-release capabilities, two major approaches can be employed. One method to control
292 the release of guest molecules is the attachment of drugs to the MSNs surface through stimulus-
293 responsive linkages. Due to the differentiated pathologies in the cancer medium, different
294 internal stimuli (i.e., pH, enzyme, and redox) can be used to stimulate the release of a drug.
295 Besides, external stimuli (i.e., temperature, light, magnet, and ultrasound) can also be utilized to
296 enable the MSNs responsiveness ability (Table 2, Figure 4) (Aznar et al., 2009; Climent et al.,
297 2009; Lai et al., 2003; Lee et al., 2010; Saint-Cricq et al., 2015; Zhu et al., 2009). Another
298 approach named "capping" or "gating" includes the joining of organic molecules at the pore
299 opening thereby inhibiting the release of a drug that exists in the pore. "Nanovalves" can be
300 connected to the pore openings to present close and open functions for drugs loaded in the
301 mesopores. The chemotherapeutic agents stored in the mesopores thus remain inside NPs by the
302 closure of the nanovalves. The release of stored chemotherapeutics can therefore be achieved by
303 opening the nanovalves. To date, different capping (gating) materials such as Au (Yoon et al.,
304 2003), rotaxanes and pseudorotaxanes (Gayam and Wu, 2014), metal NPs (Chen et al., 2011),
305 dendrimers (Nadrah et al., 2013b), and proteins (Schlossbauer et al., 2009) have been developed.

306

307 **3.2.1 pH-Responsive Systems**

308 The pH-sensitive formulations have been designed in order to overcome the deficiency of
309 conventional drug formulations. Generally, pH triggering is the common method used to control
310 drug release. Because of the acute disorganized vasculature, hypoxia, and raised interstitial
311 pressure in the internal milieu of tumors, increased glucose consumption and production of
312 additional metabolites -mostly lactic acid- (known as Warburg's hypothesis), it results in creating
313 tumor acidosis. The pH in tumor tissues is less than that of normal tissues (Liberti and Locasale,
314 2016). This property provides massive benefits with regards to targeted delivery to cancer cells.
315 The pH-sensitive binders are a class of chemically degradable binders that can be attached to
316 MSN-based nanocarriers for controlled drug release in cancer cells (Casasús et al., 2004).
317 Blocking the MSNs pores with a non-covalently bonded pH-sensitive polymer is an efficient
318 method in controlling drug release. At low pHs, polymers can be separated from the particles,
319 and thereby the release of a drug at a specific acidic tumor site can be achieved. Among these
320 methods, using polyelectrolyte multilayers (PEMs) is one of the main approaches to control the
321 release of drugs. PEMs are polymers whose repeating units bear electrolyte groups. They are
322 typically attached to the MSNs surface to work as a pH-triggered release system by
323 conformational transition under various pHs (Yang et al., 2014b). The polyelectrolytes strongly
324 coil around the MSNs thus inhibiting the drug release under a weakly basic or neutral milieu. For
325 instance, to induce a pH-sensitive swelling and de-swelling capability to MSNs for controlling
326 the drug release rate, MSNs were modified with PEMs of poly (allylamine hydrochloride)
327 (PAH)/sodium polystyrene sulfonate (Tamanna et al., 2015). Moreover, various functional
328 groups have been employed to be used as attachments to MSNs for pH-triggered drug release.

For example, Che and coworkers have designed an MSN-based pH-triggered delivery system by coordinating the bonding of functional groups on the pores with drugs and metal ions (Zheng et al., 2011). This "host-metal-guest" framework showed significant constancy over fast pH responsivity and was identified as a novel approach for pH-triggered release in cancer treatment. Lee *et al.* prepared calcium phosphate capped-MSNs as a DDS that releases drugs under acidic pH (Zheng et al., 2011).

Mu *et al.* fabricated a pH-sensitive MSN-based DDS modified with poly (L-histidine) (PLH) and PEG for tumor-specific release of sorafenib. The PLH is pH-dependent and therefore, the coating showed an "on-off" mechanism of release. The NPs exhibited negligible hemolysis activity, good anti-proliferative activity, and inhibited tumor growth (Mu et al., 2017).

Huang *et al.* prepared MSNs that were functionalized via polydopamine (PDA) for the extended release of a cationic amphiphilic drug, desipramine (DES). MSNs-DES-PDA had a strong pH-sensitivity pattern. The DES release patterns from MSNs-DES and MSNs-DES-PDA were dramatically different with the release of drugs from MSNs-DES-PDA increasing with a rising increase in acidity. The *in vitro* cytotoxicity investigation indicated that compared with the free DES, MSNs-DES-PDA had a higher cytotoxicity effect on cells. The IC50 values of HeLa cells treated with MSNs-DES-PDA at 24 h and 48 h were 7.21 ± 0.36 and 1.96 ± 0.13 µg/ml respectively versus those of the free DES (22.31 ± 1.12 and 8.59 ± 0.56 µg/ml respectively), suggesting that the formers were 3.09- and 4.38-fold effective. It was therefore concluded that MSNs-DES-PDA had a higher cytotoxicity effect against HeLa cells because of the sustained drug release rate (Chang et al., 2016).

Saroj *et al.* synthesized pH-responsive PAA-MSN and Etoposide (ETS) and introduced them into PAA-caged MSNs for cancer therapy. MSN-PAA was investigated as carriers for loading

and for the controlled release profile of ETS at various pHs. The PAA-MSNs had a high loading content of 20.19%. The release profile of ETS-MSN-PAA and ETS-MSN was measured as a function of pH and time. The cumulative drug release percentage at different pH values of 5.6, 6.8, and 7.4 was calculated to be 85%, 70.72%, and 36.21%, respectively. The maximum drug release was observed at the lowest pH of 5.6. This was because PAA was protonated at lower pH values (5.6 and 6.8), which eventually resulted in the detachment of strong electrostatic forces between PAA and ETS. The strong electrostatic forces with PAA prevented drug release at higher pH. The results of the MTT (3-(4,5-dimethylthiazol-2-yl)-2,5 diphenyl tetrazolium bromide) assay revealed that the drug-loaded MSN-PAA NPs were more cytotoxic against PC-3 and LNCaP prostate cancer cell lines, compared to the free ETS (Saroj and Rajput, 2018).

dos Apostolos *et al.* synthesized Cu-containing mesoporous silica/hydroxyapatite-based nanocomposites which were modified with the pH-sensitive polymer, methacrylic acid (MAA), and tetraethylene glycol dimethacrylate as a linker. Methotrexate (MTX) can be presented in the anionic and cationic forms, related to the protonated amino group. At pH 5, the MAA is in its non-ionized form. The results proved that the existence of hydrogen bonds between the polymer and the cationic group of MTX could control the release of MTX at pH 5. Although the synthesized NPs exhibited 70 times lower MTX than the free drug, they showed a high cytotoxic effect for both cells when in vitro cytotoxic activity of the NPs in fibroblast and Saos-2 cells were investigated (dos Apostolos et al., 2019).

3.2.2 Redox-Sensitive Systems

The potential of redox occurs generally in the tumor environment and has been regarded as a viable biomarker for drug release. Redox-responsive vectors can reply to the different

concentrations of glutathione (GSH) between extracellular environments equal to 10 μM and intracellular environments in the range of 1-10 mM (Zheng et al., 2011). The specific redox potential difference between the inside and outside of cells is referred to as the trigger release of particulate drugs within the intracellular domain of the tumor environment (internal trigger). The most important aspect of disulfide bonds is their cleavage, which occurs in the intracellular space with a comparatively high concentration of GSH. Therefore, various redox-responsive cargo release systems have been developed. These compose of various nanocaps, for example, CdS (Lai et al., 2003), Fe_3O_4 (Giri et al., 2005), gold NPs (Torney et al., 2007), and biomolecules that are covalently attached to the MSNs. The disulfide bond is used as a redox-responsive linkage between nanocaps and MSNs. The disulfide bridge is cleaved at high intracellular GSH concentrations creating two thiol groups at the targeted tumor site. These phenomena may lead GSH to operate as a reduction agent (Nadrah et al., 2013a). Many *in vitro* investigations have demonstrated that mercaptoethanol and dithiothreitol (DTT) act as disulfide-reducing agents to confirm the redox potential mechanism. For instance, Liu *et al.* synthesized crosslinked poly(N-acryloxysuccinimide) connected to the MSNs pore gateway (Nadrah et al., 2013a). DTT cleaved the disulfide bridges of the cystamine which resulted in the spatial disruption (and weakening) of the polymer system and caused the redox-triggered drug release. Besides the polymers, Lin *et al.* attached the inorganic iron oxide NPs as caps to MSNs (Giri et al., 2005). These Fe_3O_4-capped MSN-based nanocarriers exhibited "zero-release" before reaching cells of the target tissues with the cargo being released by dissociation internalization. A study on a redox-responsive delivery system showed that a disulfide bridge was used to attach a mercapto-containing drug, 6-mercaptopurine, to mercapto-functionalized MSNs (Zhao et al., 2014a). Also, by a simple modified grafting process, various anticancer drugs such as cisplatin and DOX can

accept a mercapto group and then be covalently grafted to MSNs by a disulfide bond (Ahn et al., 2013; Wang et al., 2013). Many redox-responsive MSN-based platforms hold the cargoes within their mesopores with gatekeepers grafted on their surfaces through disulfide bonds. These systems can be fabricated by employing heparin (Dai et al., 2014), collagen (Luo et al., 2011), PEG (Wang et al., 2015), cytochrome C (Cyt C) (Zhang et al., 2014), etc. as end-capping agents for redox-sensitive MSNs. Cyt C can attach to apoptotic protease activating factor (Apaf-1), which induces the caspase cascade pathway to result in cell apoptosis (Matapurkar and Lazebnik, 2006).

In a redox-responsive DOX/siRNA co-delivery system, the surface of MSNs was decorated with the adamantane (Ad) units via a disulfide bond (Ma et al., 2014). The DOX was blocked inside the mesopores through the formation of a host-guest complex among Ad and ethylenediamine-modified α-cyclodextrin (α-CD). The amine groups could form complexes with siRNA via electrostatic interaction. Due to the cleavage of disulfide bonds, a high amount of GSH mediated reduced environment for triggering DOX/siRNA release. The simultaneous delivery of siRNA and DOX by prepared NPs could enhance the cytotoxicity against HeLa cells and significantly inhibit the growth of liver tumors (P=0.0291).

3.2.3 Enzyme-Triggered Systems

The control of anticancer drug release based on enzyme-trigger is obtained due to good biocompatibility, and specific and high biological enzymatic activity. MSNs have been used to protect anticancer cargos by blocking the pores using capping agents such as proteins, peptides, and lipids which can be removed in the presence of enzymes as stimuli (Li et al., 2019). Matrix metalloproteinases (MMPs) are a type of proteases that destroy the extracellular matrix

components. The overexpression of these materials have been observed in many cancer types. They are overexpressed in some tumor microenvironments and have been exposed to improve the migration of tumor cells from primary cancer throughout metastasis (Du et al., 2015; Overall and Kleifeld, 2006). For example, gelatin, as an MMP2-sensitive linker, has been used for enzyme-triggered drug delivery, indicating a comparatively higher degree of hydrolyzation and controllable drug release kinetics (Zou et al., 2015).

The MSN-based enzyme-triggered systems can be applied for drug delivery in cancer treatment studies. Some biopolymers such as chondroitin sulfate and HA have been reported as multifunctional capping agents for the retention of drugs in MSNs, targeting cells or organs, and bio-responsive release of the drug. CD_{44} biomarkers in tumor cells are overexpressed by chondroitin sulfate capping agents causing a slower encapsulated drug release followed by trigging with enzymes such as lysosomal hyaluronidase which is abundant within tumor cells (Li et al., 2021). For instance, an MSN-based enzyme-sensitive DDS was developed for targeting cancer cells and mitochondria (Naz et al., 2019). Triphenylphosphine (TPP), a mitochondria-targeting compound, was attached to the surface of MSNs with DOX loaded into the mesopores. HA capped on the surface of MSNs and imparted a powerful sealing ability in normal cells while enhancing selective uptake by cancer cells via CD_{44} receptor-mediated endocytosis processes. Furthermore, the HA-modified NPs demonstrated enzyme-responsive DOX release under the degradation of the overexpressed hyaluronidase in the cancer cells. In addition, the existence of TPP enabled the DDS to target mitochondria and release DOX at the subcellular organelle (Naz et al., 2019).

3.2.4 Light-Activated Systems

Leveraging on the different signs of progress in PDT therapeutic agents, light irradiation is used

to trigger the drug release operatively for site-specific release of drugs. O-nitrobenzyl ester, thymine, coumarin, azobenzene, and aluminum phthalocyanine disulfonate as photochemical responsive bonders are common capping agents for efficient light-triggered release from MSNs (Murugan et al., 2021).

Photo-induced hyperthermia, which is relatively non-invasive is utilized as a trigger for controlled drug delivery in cancer therapy. The benefits of the application of light rely on its low toxicity, simple usage, and fine position of the focalized light in the right position. However, the chief disadvantage is its poor and slow penetration (Ferris et al., 2009). The initial light-triggered release system based on MSNs was investigated by the Tanaka group (Mal et al., 2003). They synthesized a UV-light sensitive smart drug delivery containing coumarin derivatives attached to the pore walls to control the release of the drug. Li et al. designed a red-light responsive MSN-based nanosystem and employed a cyanine dye that was linked to the surface of MSN-doped with DOX, which was further wrapped by PEG. Upon red light (650 nm) irradiation, the photolabile cyanine-azide linker was cleaved and led to the dePEGylation of the nanocarrier. The encapsulated DOX could then be effectively released in xenografted 4T1 tumor-bearing BALB/c mice (Li et al., 2020).

Under near-infrared (NIR) light, the tissue exhibits deep penetration but low absorbance. A broad type of photothermal NPs show poor absorption within NIR ranging from 750 nm to 2500 nm. The photon energy absorption is transformed into warmth with great capability. Heat induces a temperature rise in the target tissue, which leads to a destruction of the endosome and an improvement in the endosomal escape of the nanocarriers and thus an increase in membrane

permeability (Martinez et al., 2010).

Au nanostructures and carbon based materials (Monem et al., 2014), copper sulfide (CuS) NPs

(Wu et al., 2014) and Pd nanosheets (Zhao et al., 2014b) have been employed to prepare mesoporous silica platforms for chemo-photothermal therapy (PTT) (Gao et al., 2020). Zheng *et al.* used Ag NPs as the capping agent for MSN-coated gold nanorods for photothermal and photodynamic cancer therapy (Zhang et al., 2015b). Upon NIR irradiation, the photothermal effect of Au nanorods led to a fast increase in the local temperature, consequently, causing improved cell cytotoxicity. It can therefore be concluded that photothermal and photodynamic therapy have a synergistic effect on killing tumor cells. CuS NPs, as a cap, were bonded to MSNs through two complementary oligonucleotides to inhibit the premature release of DOX from MSNs (Liu et al., 2011a). Under NIR irradiation, the temperature increased, which caused the release of DOX. In another example, a gold nanoshell was attached to MSNs. NIR laser irradiation increased temperature and this hyperthermia was a marker for the severe toxicity of cells. Under the NIR irradiation, the localized generated heat induced the dehybridization of the DNA duplex and unlocked the pores which resulted in the quick release of DOX.

3.2.5 Magnetically-Triggered Systems

The use of magnetic field as an external stimuli to generate controlled DDSs has the advantage of high tissue penetration capability without damaging the surrounding tissues. To achieve this goal, a specific kind of NP that possesses an iron oxide magnetic core is used (Liong et al., 2008). The large amount of pure magnetic NPs is synthesized in organic solvents and indicates low aqueous stable dispersion. These are normally in an aggregated state but not segregated (Pan et al., 2017). The aggregation can reduce the heating efficiency of the magnetic

NPs (Kumar et al., 2017). In clinical applications, the magnetic field can trigger the release of drugs and penetrate living organisms. Considerable attention has been paid to the encapsulation

of superparamagnetic iron oxide nanocrystals ranging in diameter from 5 to 10 nm into a silica matrix. Magnetic MSN-based delivery systems, due to the intrinsic properties of it being magnetic means it can be utilized in MRI and the production of thermal energy can be used to induce the enhanced and controlled release of encapsulated drugs.

For example, Chen *et al.* synthesized monodispersed Fe_3O_4-capped MSNs via chemical bonding. The incorporation of Fe_3O_4 into the MSNs indicated a higher accumulation of nanocarriers in the cancer cells under external magnetic field stimulation as compared to bare MSNs. The drug toxicity and uptake of MSN@Fe_3O_4 nano-complexes were affected by the distance between magnet and cells thus exhibiting their efficiency in magnetic drug targeting (Li et al., 2016; Yang et al., 2014a). Li *et al.* fabricated mesoporous silica shell-coated Fe_3O_4-Au core-shell nanocomposites (Fe_3O_4@Au@mSiO_2). MSNs without magnetic induction showed a 37.5% of Au concentration in HeLa cells uptake. Under the magnetic field for 2 h, the amount of Au increased to 63.8% (Li et al., 2014).

3.2.6 Temperature-Responsive Systems

Amongst external stimuli employed for DDSs, temperature-sensitive DDSs have many advantages due to their passive targeting capability, regulating the phase transition temperatures, and flexibility in design (Thrall et al., 1986). Polymers like poly(*N*-isopropyl acrylamide) (PNIPAAM), which possess temperature-sensitive properties, can be connected to the MSNs for controlling/modulating the release of drugs. Such polymers have a low critical solution temperature (LCST) factor. At temperatures below the LCST, PNIPAAM becomes soluble and

moves to the swelling state because of the strong hydrogen bonding between water molecules and polymer chains. Above the LCST, the hydrogen bonds break, leading to insolubility and collapse of the PNIPAAM thus causing the pore opening and drug release (Colilla et al., 2013). Pure PNIPAAM indicates LCST at ~32°C which is not sufficient for the DDS, while the temperature of the body is higher, which induces the pores to open. The copolymerization of PNIPAAM with other monomers, for example, N-isopropylmethacrylamide or acrylamide (Nagase et al., 2007; Zintchenko et al., 2006) leads to an increase (to ~37 °C) in the LCST (Hoare et al., 2009; Keerl et al., 2008).

The surface-initiated atom transfer radical polymerization method was used by Dargaville *et al.* to attach PNIPAAM to the porous silicon materials surface (Dargaville et al., 2013). The composite indicated high drug loading capacity and unique controlled drug release property.

Baeza *et al.* designed a new nanodevice to control the small molecules and protein release based on the alternating magnetic field (Baeza et al., 2012). This MSN-based nanosystem is composed of iron oxide NPs encapsulated in the silica matrix and a thermo-responsive copolymer of PEI/PNIPAM, which was grafted on the outer surface of MSNs. Thermo-responsive polymers were used as gatekeepers to block the pores and to link proteins to the polymer shell *via* hydrogen bonding and electrostatic interactions. This technique inhibited uncontrolled drug release at low temperatures and when temperature increased (35-40 °C), the entrapped molecules were released (Baeza et al., 2012).

Other temperature-sensitive products such as DNA or lipids have been used in clinical applications. Schlossbauer *et al.* indicated that the molecular valve of the double-stranded DNA capped MSNs were opened by melting the DNA strand at the specific melting temperature of the oligonucleotide, which led to the controlled release of fluorescein from the pores (Schlossbauer

et al., 2010). Schlossbauer *et al.* attached biotin-labeled DNA strands to the outer surface of MSNs and regulated the pore opening temperature through the length of DNA strands

(Schlossbauer et al., 2010). Martelli *et al.* showed that coiled-coil peptide motifs can be used as a temperature-responsive cap to control drug release in MSNs (Martelli et al., 2013). These gatekeeper materials are biodegradable, biocompatible, and non-toxic which makes them a good choice for clinical carcinoma treatment.

3.2.7 Ultrasound-Triggered Systems

Ultrasonic (US) response is an effective external trigger for delivery of cargo at the desired site because of features such as the absence of ionizing radiations, non-invasiveness cycles and exposure time, cost-effectiveness, and safety in the clinic. High-frequency ultrasound has got many potential applications in nanomedicine because of its ability to deliver local therapies without any damage to normal tissues (Sirsi and Borden, 2014). Cavitation and heat are two unwanted effects of ultrasound technology that have been harnessed in the delivery of drugs. Researchers have designed encapsulated microbubbles (MBs) with MSNs nanosystems to load the drug in MBs for region targeting under image monitoring of US (Bae et al., 2011). Nonlinear wave propagation in tissue can provoke many physical impacts which can be utilized as US-triggered drug release. The mechanical and thermal properties of US have been applied to trigger the drug release from various nanocarriers.

For instance, Amin *et al.* developed a US-responsive DDS composed of lipid-coated MSNs for avoiding premature release as well as triggered drug release at the target site (Amin et al., 2021). DOX, as an anticancer drug, and perfluoropentane (PFP) as a US responsive agent, were encapsulated inside the MSN pores. The lipid layer improved the cellular uptake and also acted

559 as a gatekeeper at the pore openings to avoid premature release. Upon US irradiation, the liquid-
560 gas phase transition of PFP led to the rupture of the lipid coating which resulted in a triggered

561 drug release (Figure 5) (Amin et al., 2021).
562
563 **3.3 Multi-Stimuli Responsive MSNs**
564 Controlling the precise delivery of therapeutics in a particular part of the body can be achieved
565 by designing delivery systems triggered by multiple stimuli that can work synergistically to
566 ensure the release of the drug only in the target tissue or cells. The versatility and
567 functionalization capability of MSNs means the insertion of at least two kinds of responsive
568 moieties or functional groups in the same nanodevice is possible. The pore caps may thus be
569 opened either by one or another stimuli or simultaneously by both. It can also be possible to
570 design a stimuli cascade in which one stimulus triggers the unblocking process of MSNs or leads
571 to the release of various payloads in a sequential manner.
572 Zhu *et al.* synthesized graphene quantum dots (GQDs) caped MSNs for chemo-PTT. The GQD-
573 MSNs showed pH and temperature-responsive release behavior and under NIR irradiation,
574 effectively produced heat to destroy tumor cells. DOX-loaded GQD-MSNs induced higher
575 uptake efficiency, cytotoxicity, and increased intracellular accumulation in 4T1 breast cancer
576 cells (Sasikala et al., 2016).
577 Luo *et al.* designed a multifunctional MSN-based enveloped nanosystem for the co-delivery of
578 the antineoplastic drug, topotecan (TPT), and therapeutic peptide (TPep) to tumor cells (Luo et
579 al., 2014). TPT was entrapped in the mesopores of MSNs and the mitochondria-targeted
580 therapeutic molecule, TPep, was attached to the surface of MSNs by a disulfide bond. The NPs
581 were modified with PEG-poly(L-lysine) (PLL) and 2,3-dimethylmaleic anhydride (DMA)

582 moieties and were introduced into the polymeric chains. This made the system sensitive to the
583 pH alteration thus making the cellular uptake of the enveloped NPs at pH 6.8 much more than

584 that of the NPs at neutral pH. After internalization by the cancer cells, the disulfide bonds
585 cleaved in the presence of intracellular GSH, TPT, and TPep could be released from the MSNs.
586 This in turn destroyed both the nucleus and tumor mitochondria respectively hence
587 demonstrating complementary synergistic therapeutic effects (Figure 6) (Luo et al., 2014).
588 A dual responsive MSN with poly (NIPAM-co-MA) polymer and a lipid coating was fabricated
589 by Feng *et al.* to co-deliver berberine and evodiamine. This pH and the temperature-responsive
590 system showed that the cumulative release of evodiamine and berberine was 89.01% and 57.98%
591 respectively at a pH value of 5 and a high temperature (~41°C) which simulated the lysosome in
592 the tumor cell. Also, NPs showed excellent synergistic therapeutic effects *in vitro* and an
593 enhanced rate of apoptosis to suppress tumor growth in mice (Feng et al., 2018).
594 Because reactive oxygen species (ROS) levels in tumor cells are much higher than in normal
595 cells, ROS-triggered drug release has indicated officious cancer treatment (Liu et al., 2019). Yu
596 *et al.* used a temperature and ROS dual responsive polymer, 4-(4,4,5,5-tetramethyl-1,3,2-
597 dioxaborolan-2-yl) benzyl acrylate, to modify MSNs for the delivery of DOX to cancer cells. A
598 high drug-loading content was attained at low temperature and the pore-blocking was obtained
599 by raising the temperature (37 °C). A fast drug release was achieved in the existence of H_2O_2
600 because of the coated-polymer phase transition from hydrophobic to hydrophilic, whereas there
601 was no burst release under physiological conditions (Yu et al., 2018a).
602 In a research study, the thermoresponsive polymer MEO_2MA and 2-(2-methoxyethoxy) ethyl
603 methacrylate were combined with an US-responsive monomer (THPMA) to prepare copolymers
604 sensitive to heat and US (Paris et al., 2015). Grafted copolymers with MSNs facilitated an

efficient loading of drugs into the prepared nanostructures at 4 °C due to the open conformation of the thermosensitive polymer chains at this temperature. At higher temperatures (37 °C), the thermosensitive polymer collapsed to close the pore entrances. Under US irradiation, the sensitive polymer changed its hydrophobicity and adopted a coil-like conformation that opened the gates and released the drug cargo. This dual responsivity allowed the NPs to carry and control drug release which is significant in transporting cytotoxic drugs to treat cancer.

Furthermore, if tumor-targeting ligands are attached to the gatekeepers, stimuli-responsive DDs for selective delivery to specific cancer cells and highly controllable drug release can be obtained. For example, Zhang et al. prepared multifunctional MSNs for the targeted delivery of DOX to cancer cells. The surface of the MSNs was modified with amino β-cyclodextrin (β-CD) rings *via* disulfide bonds. The amino β-CD ring was utilized as a cap to block drug molecules within the mesopores. In this study, PEG-modified with Ad units and folate moieties were successfully attached to the MSNs *via* the Ad/β-CD complexation. The obtained multifunctional MSNs including the folate targeting units were trapped efficiently by folate receptor-rich HeLa cancer cells via receptor-mediated endocytosis. Under the same conditions, the folate-receptor-poor human embryonic kidney 293 normal cells presented less endocytosis. The main cellular uptake mechanism was endocytosis which could lead to the release of loaded DOX into the cancer cells triggered through endosomal acidic pH. Following the endosomal escape of NPs and its transfer to the cytoplasm of cancer cells, a high amount of GSH could be trapped in the cytoplasm and result in the elimination of the β-CD capping rings through the cleavage of disulfide bonds to enhance further drug release in the cytoplasm of cancer cells. These drug-loaded multifunctional MSNs could considerably reduce the growth of cancer cells due to the high potency of cellular uptake via receptor-mediated endocytosis and stimuli-triggered drug

release (Zhang et al., 2012). Some of the different materials that have been attached to MSNs for different applications in cancer treatment are shown in Table 3.

3.4 Overcoming Multidrug Resistance (MDR)

One of the biggest barriers to cancer chemotherapy is the emergence of MDR, which severely impedes the efficacy of chemotherapeutic agents. Drug resistance in tumor tissues is a complex process that involves multiple cellular mechanisms (Kankala et al., 2017). MDR can be commonly classified into two groups; pump and non-pump resistance. Pump resistance is the overexpression of drug efflux pumps such as multidrug resistance protein (MRP1) and P-glycoprotein (P-gp). These expel several anticancer drugs out of cancerous cells and thereby reduce the intracellular drug concentration. The major mechanism of non-pump resistance is the activation of the cellular antiapoptotic defense system, such as the drug-induced expression of B-cell lymphoma-2 (BCL-2) protein, which leads to a reduction in drug sensitivity. Furthermore, there is mutual interaction between these two resistance mechanisms (Tanwar et al., 2014). To overcome drug resistance, various design strategies based on the outstanding features of MSNs have been employed. The MSNs nanostructures can facilitate cellular uptake, enhance the accumulation of drugs in the tumor region, and improve antitumor efficacy (He and Shi, 2014). MSNs can co-deliver various agents, such as antitumor drugs and MDR reversal agents. For instance, to tackle the MDR of MCF-7/ADR cells, Jia et al. synthesized MSNs for the co-delivery of tetrandrine (TET) and paclitaxel (PTX) (Jia et al., 2015). The efflux of P-gp can be inhibited by TET and thereby result in the enhancement of the antitumor activity of PTX. Several research groups have utilized MSNs to deliver anticancer drugs and nucleic acids. Nucleic acids in combination with chemotherapeutics provide the opportunity for silencing specific genes

involved in drug resistance such as the drug efflux transporter gene P-gp and antiapoptotic protein gene BCL-2. Thus, the intracellular drug concentration needed for effective cytotoxicity and apoptosis can be restored (Famta et al., 2021; Torres-Martinez et al., 2021). In another study, Meng *et al.* modified MSNs to effectively deliver P-gp siRNA and anticancer agent DOX to MDR cancerous cells (KB-V1cell line) (Meng et al., 2010). It was perceived that the dual delivery of siRNA and DOX improved the intracellular and intranuclear drug concentrations more than the free DOX or DOX-loaded MSNs without siRNA.

It has been reported that an ideal nuclear-targeted nanoparticulate DDS can help overcome MDR (Pan et al., 2014). To construct a nuclear-targeted anticancer DDS, MSNs can be modified with a Trans-Activator Transcription (TAT) peptide. For instance, Pan et al. developed an active nuclear-targeted DDS by attaching TAT peptides onto the MSNs for MDR circumvention in cancer cells (Pan et al., 2013). The attachment of the TAT peptide facilitated direct drug release in the nucleoplasm by the nuclear pore complex and subsequent intranuclear binding of the MSNs-TAT. Direct intranuclear drug delivery of DOX was more efficient in overcoming MDR of MCF-7/ADR cancer cells by improving the intranuclear and intracellular drug concentrations compared to the free drug or untargeted MSNs. Thus, direct nuclear-targeted drug delivery may help the drugs bypass the P-gp drug efflux pump by reducing ATP levels, overcoming the MDR, and increasing apoptotic signaling of MCF-7/ADR cells (Figure 7) (Pan et al., 2013).

In another study, MSNs were modified with Alpha-tocopheryl polyethylene glycol succinate (TPGS) for multidrug-resistant lung cancer treatment. New generation coatings TPGS were utilized to reduce P-gp meditated process multidrug resistance in the cancer cells. Enhanced cellular uptake in drug-resistant A549 cells was obtained from the MSNs coated TPGS, therefore proving the relapse of drug resistance (Cheng et al., 2017).

4. Diagnostic Applications of MSNs

Non-invasive imaging techniques such as MRI, optical imaging (OI), positron emission tomography (PET), computed tomography (CT), and ultrasound (US) represent a powerful asset for the diagnosis of diseases. Imaging clarity can be remarkably enhanced by using an associated contrast agent (Peng et al., 2021). Due to the poor solubility and low fluorescence quantum yield in physiological solutions, the biological applications of fluorescent dyes are limited and they are not the favored selection for clinical imaging (Yuan et al., 2020). Compared to conventional molecular analogs, MSNs as flexible imaging platforms can be attached to imaging agents and provide considerable advantages (Kankala et al., 2019).

4.1 Magnetic Resonance Imaging

MRI is one of the most powerful imaging modalities, which can identify many disease states due to its high 3D resolution, penetration depth, and convenience. MRI however suffers from intrinsic low sensitivity. In order to overcome this obstacle, contrast agents can be used (Wahsner et al., 2018). Based on the generated contrast enhancement, MRI contrast agents are classified as being longitudinal (T_1) or transverse relaxation (T_2). T_1 (positive contrast agents) brighten the region of interest and T_2 (negative contrast agents) darken the desired area (Ni et al., 2017).

MSNs with the ability to shorten longitudinal relaxation rates can be achieved by the formation of a core/shell structure comprising a mesoporous silica shell and a magnetic core. For example, Liu et al. investigated the long-term usefulness/contrast improvement of Mag-Dye@MSNs with magnetic and optical features, both upon intravenous injection and grafting of Mag-Dye@MSN-labeled human mesenchymal stem cells at the brain olfactory cortex through MRI (Liu et al.,

2008). In this study, the reticuloendothelial system (RES) caused the accumulation of Mag-Dye@MSNs into organs, particularly in the spleen and the liver. The NPs were visualized in the liver for 90 days, demonstrating that the ratio of signal-to-noise improved after 3 months. This indicated that the Mag-Dye@MSNs were stable and not simply eliminated from the body.

4.2 Optical Imaging

OI is a non-invasive and non-ionizing imaging technique, which provides excellent spatial resolution and versatility. Various luminescent materials (e.g., luminescent inorganic nanocrystals, organic fluorophores, etc.) have been widely studied, however, some of them have limitations. For example, organic fluorophores suffer from poor photostability and rapid photobleaching. Moreover, most of the nanosized luminescent materials have colloidal stability or present serious concerns for toxicity (Sun et al., 2021). To tackle these aforementioned problems, these luminescent materials can be encapsulated into the MSN scaffold. For instance, Xie *et al.* functionalized the surface of MSN with carboxyl groups to covalently conjugate fluorescent probes (Xie et al., 2013). Cy5 was conjugated on the surface of carboxyl-modified MSNs to obtain Cy5@MSN/COOH. *In vitro* cellular uptake studies using MCF-7 cells indicated that Cy5@MSN/COOH were internalized by the cells and were located in the cytoplasm. *In vivo* imaging experiments were conducted in MCF-7 tumor xenograft mice. An obvious and strong fluorescent signal was observed in the tumor region after the injection of Cy5@MSN/COOH into the subcutaneous tumor of the mouse. After 96 h post-injection, the fluorescent signal was still bright, which indicated that Cy5@MSN/COOH has great potential for *in vivo* tumor imaging.

720 **4.3 Computed Tomography**

721 CT imaging comprises 3D anatomical imaging based on differences in the X-ray attenuation

722 coefficient. It is an important modality in diagnostics, which has low cost and high spatial
723 resolution (Han et al., 2019). Current CT contrast agents are based on iodine analogs that suffer
724 from anaphylaxis, potential renal toxicity, and poor blood circulation time. Encapsulation of
725 these CT agents within the MSN structure can facilitate their use and also improve the retention
726 time and biocompatibility. In addition, compared to iodine analogs, bismuth and gold possess
727 improved X-ray attenuation meaninga lower concentration required to be utilized *in vivo* (Xue et
728 al., 2014).

729 MSN-coated gold NPs were fabricated by Song *et al.* for fluorescence/CT imaging (Song et al.,
730 2015). NIR fluorescent dyes were encapsulated into MSNs shells for fluorescent imaging
731 through electrostatic interactions. The *in vitro* CT imaging of MSNs-Au at different
732 concentrations showed different CT values that increased in linearly with the increase of Au
733 concentration. The *in vivo* CT imaging studies were conducted by the injection of MSNs-Au into
734 male nude mice through the tail vein within 4 h. The high-resolution obtained images revealed
735 that the MSNs-Au were mainly distributed in the liver and spleen tissues.

736

737 **4.4 Positron Emission Tomography**

738 It is well-perceived that PET is the most sensitive imaging modality which can provide
739 information at a molecular level in living systems (Goel et al., 2017). The visualization of *in vivo*
740 biological processes using PET requires the preparation of specific radiolabeled probes.
741 Moreover, PET has limitless penetration depth and a wide range of clinically applicable probes.
742 However, radiolabeled molecules evoke concerns about their long-term *in vivo* integrity and

743 stability. Thus, it is a key improvement to develop MSN-based carriers for the application of
744 positron emitting radionuclides with longer half-lives. The conjugation of radionuclides with

745 long half-lives, including zirconium-89 (^{89}Zr) or copper-64 (^{64}Cu) in MSNs have been
746 investigated by several research groups (Chen et al., 2015a; Chen et al., 2014a; Miller et al.,
747 2014).
748 Short half-life radionuclides have also been incorporated into MSNs by efficient
749 loading/conjugating. For instance, Fluorine-18 (^{18}F) ($T_{1/2}$ = 109.771 min)-labeled MSNs were
750 described by Jeong *et al.* for *in vivo* imaging, with conjugation obtained using a strain-promoted
751 alkyne azide cycloaddition (SPAAC) reaction (Jeong et al., 2019). The surface of PEGylated
752 MSNs was modified by cyclooctyne and intravenously injected into the tumor-bearing mice. A
753 few days later, the NPs functionalized with the ^{18}F-labelled azide species were injected. The
754 accumulation of radiolabelled NPs in the tumor region was observed and visualized by PET
755 imaging.
756
757 **4.5 Ultrasound Imaging**
758 US imaging as a simple, flexible, non-invasive, and inexpensive modality is the primary and
759 widely used technique for screening many different diseases (Kiessling et al., 2014).
760 Microbubbles produced by agitating saline have been utilized as a contrast agent for US imaging
761 (Liu et al., 2017). These contrast agent microbubbles with acoustic behavior coupled with MSNs
762 have been broadly investigated for US imaging. For example, an MSN-based enhancement agent
763 for ultrasound imaging developed by Wang et al. and loaded with a temperature-sensitive
764 compound, perfluorohexane (PFH), as a bubble generator (Wang et al., 2012). Upon ultrasound
765 exposure, the liquid PFH vaporized into a large number of small bubbles. PFH bubbles generated

heat to the MSNs-PFH (6 mg mL^{-1}) at 70 °C. While the unmodified MSNs did not generate any microbubbles in the overall heated area, numerous microbubbles were observed after the heat treatment of MSNs-PFH. Phosphate buffered saline (control), MSNs, and MSNs-PFH were separately injected into excised bovine livers and then exposed to ultrasonic irradiation at 70 W for 10 s. The results showed that MSNs-PFH could be an effective diagnostic agent for ultrasound imaging due to its high physiological stability, efficient loading and release of PFH, and easy penetration through tumor tissue.

5. Theranostics applications of MSNs

The theranostics paradigm uses nanoscience to combine both diagnostic and therapeutic capabilities to form a single dose, which allows diagnosis, drug delivery, and monitoring of therapeutic response (Baeza and Vallet-Regí, 2020). Therapeutic methods including radiotherapy, photodynamic therapy, hyperthermia, chemotherapy, and nucleic acid delivery are coupled with one or more imaging agents for both *in vitro* and *in vivo* investigations. Various imaging probes such as nuclear imaging agents, fluorescent markers, and MRI contrast agents can be added to the therapeutic molecules or DDSs to obtain important information about the intracellular trafficking pathways and efficiency of delivery (Živojević et al., 2021). Moreover, to overcome undesirable differences in selectivity and biodistribution between distinct therapeutic and imaging agents, theranostics combine the functions and features of separate materials into one class. The theranostic nanomedicine has advanced abilities including multimodality diagnosis, stimuli-responsive release, targeted delivery, and sustained/controlled release in a single platform (Jafari et al., 2019). The combination of diagnosis and therapy in a single theranostic nanocarrier was achieved from the incorporation of imaging agents such as

magnetic nanocrystals (Sanson et al., 2011), molecular fluorophores (Gao et al., 2016), radionuclides (Jakobsson et al., 2019), or ultrasound contrast agents (Shi et al., 2013) into nanocarriers.

In a research study, the two-photon paracyclophane fluorophores and azobenzene stalk groups were attached to MSNs pores to be used as a nanovalve for monitoring the release of an anticancer drug (Croissant et al., 2014). The fluorescence MSNs were efficient in the imaging of the MCF-7 breast cancer cells at low power of two-photon irradiation. In the presence of high-power irradiation, the nanovalves displayed efficient two-photon triggered drug delivery in cancerous cells.

In another study, TRC105 was joined onto the surface of MSNs against CD10 to target the cancer cells as a specific vascular marker for tumor angiogenesis (Chen et al., 2014b). Compared to non-targeted controls, the obtained results proved that there was significant progress in both PET and fluorescence imaging resolution which were conducted in 4T1 murine breast tumor-bearing mice. Vascular targeting could enhance tumor accumulation two times more than passive targeting alone. In this study, TRC105 could be used as both an imaging and therapeutic agent, leading to a theranostic platform (Figure 8) (Chen et al., 2014b).

6. The Influence of Physicochemical Properties of MSNs on Biological Systems

The influence of physicochemical properties of NPs such as surface area, shape, and size on biological systems plays a pivotal role in the efficient delivery of chemotherapeutics (Kankala et al., 2020a). MSNs have a high specific surface area (>1000 m^2/g), which can be decreased by surface modification strategies such as amination or coating (Heidari et al., 2021; Van Rijt et al., 2016). The NPs with large pores (~ 10 nm) show a smaller specific surface area (Möller et al.,

2016). A larger surface area can increase the loading efficiency of therapeutic molecules. For instance, compared to the FDA approved liposomal formulation Doxil® a nearly 1000 fold amount of DOX can be loaded in MSNs (Watermann and Brieger, 2017).

Size is very important to improve the stability and blood circulation time of MSNs. It is generally recognized that the NPs with a diameter of less than 10 nm is quickly removed by the kidneys, whereas larger NPs (> 200 nm) are likely to be removed by the RES. The preferred size to ensure long circulation half-time for MSNs is therefore 50-300 nm (Vallet-Regí et al., 2022). The lower limit is set to prevent the fast-renal clearance whereas the upper limit is set to avoid embolisms due to aggregation into the capillaries and alveoli. It should be noted that MSNs with a size range of 50-100 nm exhibit optimal levels of cell internalization (Vallet-Regí, 2012).

Research indicates that the shape of MSNs can have a strong impact on their performance. It has been demonstrated that the best cellular uptake was achieved by rod-shaped MSNs, followed by spherical MSNs (Shao et al., 2017). The *in vivo* evaluation of rod-like MSNs revealed that short-rod MSNs were easily trapped in the liver while long-rod MSNs were preferentially accumulated in the spleen (Huang et al., 2011b).

The surface charge also influences the cellular uptake of MSNs. The positively-charged MSNs can be taken up faster than their negatively-charged or neutral counterparts by human cancer cells. This is due to the electrostatic interaction between the negatively-charged cellular membrane and the positively charged MSNs (Slowing et al., 2006). In a physiological environment, MSNs are coated by various serum proteins resulting in the formation of a protein corona, which changes the *in vitro* determined parameters such as size and surface charge, and thereby influences cellular uptake (Nel et al., 2009). The absorbed proteins can facilitate

clearance by the mononuclear phagocyte system (MPS). Coating the surface of MSNs with PEG can prevent this phenomenon and increase the circulation time of NPs in blood (Cauda et al., 2010a).

7. MSN Biosafety (Biocompatibility, Biodistribution, Degradation, Cytotoxicity)

The applications of MSNs in biomedical fields such as tumor targeting, drug/gene delivery, and tumor imaging have dramatically accelerated (Yanagisawa et al., 1990). Many research studies have been conducted in investigating the biosafety of MSNs. In some studies, histopathology and hematology outcomes indicated no specific toxic properties through any advanced MSNs. Some consequently confirmed the MSNs biosafety besides the MSNs biodistribution which can be valuable in producing MSN nanosystems for *in vivo* usage (Farjadian et al., 2019; He et al., 2020; Huang et al., 2011a). Despite the advancement of MSN nanotherapeutic systems, concerns about the toxicity in living systems have been presented (Asefa and Tao, 2012). Although several studies have reported the safety of silica-based materials, specifically MSNs, the experimental evidence is very ambiguous and as such, there is no common opinion on the biosafety of these nanomaterials (Fadeel and Garcia-Bennett, 2010; Lu et al., 2010). However, the biocompatibility and general behavior of MSNs can be optimized through simple modifications based on accessible conformation. This is because of their strong dependence on physicochemical properties such as surface morphologies, particle dimensions, shape, pore size, and crystallinity (Kohane and Langer, 2010). Experimental data confirm that control of particle shape and size is the basic factor in the toxicity and biodistribution of MSNs. The toxicity and safety of MSNs depends therefore on the dose of the MSNs. The surface properties of MSNs also have an

857 excessive influence on their biocompatibility and biodistribution (Croissant et al., 2018; Tozuka
858 et al., 2005).

859 Compared to traditional drug molecule carriers, MSNs have demonstrated an improvement in the
860 pharmacokinetics of therapeutic agents and therefore a reduction in toxicity by increasing their
861 concentration in the target cells (Alexis et al., 2008). Although MSNs have emerged as a
862 significant category of porous materials for use in advanced biomedical applications, their
863 interaction with the body cells is still not fully understood. The absorption and distribution of
864 MSNs into the body depend on the various routes of administration. Unlike the IV route of
865 administration, in which drug-loaded MSNs are absorbed directly into the bloodstream, in the
866 oral route of administration of MSNs, drugs must pass through the gastrointestinal (GI) tract to
867 be absorbed into the bloodstream (Fu et al., 2013). Before the biomedical application of MSNs,
868 an investigation into their total elimination from the body is warranted (Vega-Villa et al., 2008).
869 Upon the administration of MSNs in the body following different exposure routes, elimination
870 mainly occurred through both feces and urine. Previous reports indicated that after injection of
871 MSNs, about 95% of Si was discharged *via* feces and urine, which shows that it can be easily
872 expelled and degraded from the body (Lu et al., 2010; Moghaddam et al., 2019). The
873 pharmacokinetics of MSNs may be dependent on the different routes of administration.
874 Furthermore, the morphology, pore size, particle size, thermal oxidation, surface coating, surface
875 functionalization, and oxidation can directly affect the *in vivo* fate of MSNs (Croissant et al.,
876 2017).
877 The poor water solubility of hydrophobic anticancer drugs along with the unavailability of a
878 successful biocompatible delivery system are the major concerns in cancer treatment. It is
879 imperative to solve the important challenges of drugs such as their poor solubility and instability

in the aqueous environment which prevent their biomedical applications, especially for IV injection applications. Due to the poor solubility of anticancer drugs, the improvement of new approaches for these molecules without the use of organic solvents has earned considerable interest. MSNs suggest some potential capacities for improving the dissolution rate of poorly soluble drugs (Thomas et al., 2010b) by impacting the crystallinity or surface area. The pore size of MSNs is just to some extent greater than the size of the drug molecule, so, the production of a crystalline form of drugs is limited by the restricted space of the pores. The drug therefore maintains its non-crystalline (amorphous) form. In comparison with the crystalline phase, the amorphous state is identified to show higher dissolution rates (Ahuja and Pathak, 2009; Biswas, 2017; Thomas et al., 2010b).

The biodistribution of MSNs is affected by their physicochemical properties. The most significant change would be the gradual conversion of silica-based NP to polysilicic acid or silicic acid, which are non-toxic and often eliminated/absorbed from the body slowly (Gonçalves, 2018). Clinical trials mainly focus on designing highly biodegradable MSNs (Janjua et al., 2021).

The main pathway of silica toxicity is due to the interaction between the silanol groups from the surface and the membrane components which causes lysis and leakage of cellular components and finally cells death (Nash et al., 1966; Slowing et al., 2009). Compared to non-porous silica, mesoporous silica presents a less hemolytic effect (Mohammadpour et al., 2020). This could be associated with the low silanol density on the mesoporous surface (Lin and Haynes, 2010).

It has been reported that the cytotoxicity of various types of MSNs depends on the administration route instead of particle size (Hudson et al., 2008). Here, the MSNs were manufactured in various sizes by the use of neutral and cationic surfactants and their toxicity was measured in

rats. After intravenous injection with an equal dose of all MSNs types, fast death was detected (Hudson et al., 2008). Subcutaneous particle injection presented no major toxic effects. There was also no sign of size as a basic factor in the MSNs' biocompatibility in rats (Hudson et al., 2008). Another study proposed that the administration route can influence the MSNs biosafety. This shows that internalization, cellular uptake, and MSNs lifecycle are difficult routes that are not determined *via* only one parameter (Smith et al., 2008; Tallury et al., 2008).

In addition, the fate of MSNs after various administration routes should be considered. *In vivo* distribution and elimination studies have shown that MSNs *via* oral or intravenous routes are relatively safe materials for biomedical applications (Kankala et al., 2022). Fu *et al.* examined MSNs with a particle size around 110 nm in ICR (Institute of Cancer Research) mice (Fu et al., 2013). The administration of MSNs through the intravenous method led to the accumulation of MSNs in the spleen and liver at the end of 24 h and 7 days, while other routes of administration did not display any fluorescence in these tissues. At the end of 24 h and 7 days, no histopathological variations were found in the liver, spleen, kidney, and lung through various routes of exposure. The experimental data showed that MSNs were found to be well-tolerated and safe when administered through intravenous and oral methods (Fu et al., 2013; Tang et al., 2012).

Researchers have investigated the repeated and single-dose MSNs toxicity after intravenous injection in mice (Liu et al., 2011b; Narayan et al., 2018). The value of LD50 for MSNs was found to be higher than 1000 mg kg^{-1}. In the studies of single-dose toxicity, mice treated with MSNs did not survive at doses above 1280 mg kg^{-1}. Reciprocally, there were no behavioral variations or any pathological or hematological changes in the low-dose MSN-treated groups. Further studies have indicated that employing MSNs with a lipid layer can lead to development

progress in pharmacokinetics, performance, and biosafety (Souris et al., 2010). Liu et al. used macrophage cells and zebrafish embryos to test the possible hazards of various surface functionalized PEG-MSNs. Several MSNs with the same size but with various zeta potentials, a strong or weak positively-charged surface and the strong or weak negatively-charged surface were manufactured. Upon the embryos' incubation *via* 50 or 100 μg ml^{-1} of the MSNs, it was observed that the particles with strong positively-charged surfaces were uptaken through embryos and caused the death (approximately 94%). However, mortality did not happen with the embryos which were exposed to other surface-charged MSNs. These phenomena confirmed the effect of surface modifications on MSNs biosafety (Liu et al., 2015b; Sharifi et al., 2021b).

The size of pores also affects the activities of MSNs. The cytotoxicity study of non-porous and porous silica NPs offered upper hemolytic activity and cytotoxicity of non-porous silica NPs in comparison with their porous components (Lin and Haynes, 2010; Maurer-Jones et al., 2010). Many reports have suggested a relationship between the MSNs' anti-cancer potential and their pore sizes in the release of drugs (Jia et al., 2013). Compared to MSNs with large pore sizes, MSNs with smaller pore sizes have demonstrated a sustained drug delivery pattern and a more anti-cancer potential (Jia et al., 2013). Such examinations have revealed the effect of various morphologies and particle structures on biocompatibility, biodegradability, and the *in vivo/in vitro* assay of MSNs. Choosing a significant nanosystem for various biological activities is a topic of great interest in this area.

Molecular organic or inorganic doping (such as disulfides (Hadipour Moghaddam et al., 2017; Huang et al., 2017) or tetrasulfides (Chen et al., 2014d) iron (Wang et al., 2017), calcium (Hao et al., 2016), and manganese (Yu et al., 2016)) to mesoporous organosilica can control the degradation rates of MSNs. Moreover, surface modification influences the degradation rate of

MSNs. Cauda et al. reported that surface PEGylation of MSNs resulted in slower biodegradation kinetics (Cauda et al., 2010a). They examined the degradation rate of MSNs with several functional groups including phenyl, chloropropyl, and aminopropyl. The authors concluded that the degradation rate of phenyl functionalized MSNs was significantly higher than that of the chloropropyl and aminopropyl functionalized MSNs (Cauda et al., 2010b). It is well-perceived that the porous structure of MSNs greatly affects the rate of degradation. MSNs with lower porosity have a faster degradation rate.

Different degradation kinetics can be a merit for various biomedical purposes. The fast degradation rate might be beneficial in some biomedical applications in which therapeutic drugs have a short half-life, whereas, in the field of drug delivery, a slow biodegradation rate may result in controlled drug release. The direct effect of the morphology, size, and degradation environment on the degradation rate of MSNs has been examined by researchers. The obtained results revealed that the physicochemical engineering of MSNs permits adjusting the dissolution rate of silica in the biological environment for particular biomedical activities (Croissant et al., 2017).

Chen et al. confirmed that in simulated body fluid (SBF) at 37 °C, the MSNs degradation is independent of the diameters of NPs (Chen et al., 2015b). He et al. showed the impact of the surface area on the mesoporous silica degradation when three samples of MSNs with different surface areas of 958, 829, and 282 m^2 g^{-1} in SBF were compared (Li et al., 2015a). In the first 2 to 4 h, burst degradation was observed, causing 30, 70, and 90% hydrolytic degradation of silica as the surface area increased.

Cancerous cells use much more sugars, for example, glucose, at considerably higher rates, compared to normal cells. The major drawbacks, such as the absence of tumor selectivity and the

poor solubility of celastrol lead to low concentrations of the therapeutic drug in subcellular compartments of the target tissue, which in turn makes these structures excellent candidates for nanoparticulate delivery. Niemelä *et al*., utilized glucose as the high-affinity ligand on MSNs to deliver high loading capacities of celastrol-loaded MSNs to cancer cells. This resulted in minimum off-target properties on normal cells. MSNs were modified with sugar moieties in various manners: i) attached directly to the surface of MSN ii) mediated through a hyperbranched polymeric; the latter to increase the cellular uptake by producing a net positive surface charge and also to promote conjugation of sugar inactive sites. The surface modification impact on the effectiveness of target-specific antitumor properties of the particles was examined by analyzing the uptake in A549 (human lung carcinoma) and HeLa cells as models of cancer cells compared to mouse embryonic fibroblasts as normal cells (Niemelä et al., 2015).

8. Industrial Application of MSNs

The commercial transmission of knowledge mostly relies on scalability and therefore the preparation of MSNs at the production scale may be an obstacle to its industrialization. Due to their uniformity, highly particular characteristics, reproducibility, and collection, the industrial production of such products would be the biggest challenge for the pharmaceutical industry. Regarding the progressing biodegradable models, it is essential to use low-cost and eco-friendly sources of silica and organic agents, reduce the number of steps of synthetic methods, and perform synthesis under nontoxic status to address the challenges of environmental degradation (Mehmood et al., 2017). Industrial usage of MSNs progressed slowly when it was presented in the biomedical field. Biosensors were industrialized consuming mesoporous silica-based nanofibers for the Horseradish peroxide (HRP) immobilization (Patel et al., 2006). The larger

995 surface area, extreme porosity, and minor diameter of mesoporous silica nano-fibers cause the
996 HRP enzyme encapsulation. Further enzymes can be encapsulated by a similar method.

997 Yamauchi *et al.* immobilized capsaicin on the silica nano-particle surface in the presence of
998 polyamidoamine and its stimulus activation was determined by Yamauchi and co-workers
999 (Yamauchi et al., 2010). The successful encapsulation of capsaicin enlarged the stimulus activity
1000 in comparison with capsaicin alone. Although inherent toxicity is a concern with the majority of
1001 inorganic NPs, encouraging studies on the biocompatibility and effectiveness of MSNs in animal
1002 models display their incredible ability to navigate this platform to medical conditions (Narayan
1003 et al., 2018).
1004
1005 **9. Conclusions and Future Outlook**
1006 In this review, the usage of MSN-based materials with anticancer properties was discussed.
1007 MSNs serve as an excellent candidate for cancer treatment because of their unique high specific
1008 surface area and pore volume, tunable surface functionality, stability, good biocompatibility and
1009 biodegradability, and the possibility of creating hierarchical structures. Despite the major
1010 developments in the preparation and application of MSNs, many challenges remain with regards
1011 to their application, processing, and following translation before industrialization, which hinders
1012 their biomedical applications. To achieve simultaneous diagnosis and therapy as a future
1013 viewpoint, novel investigation works and studies on the MSNs should be concentrated on
1014 theranostics agents. Furthermore, care and consideration should be taken regarding the
1015 mechanisms underlying the several aspects of NPs for example, size, charge, and shape on the
1016 cellular activities in informing and designing more efficient MSN-based diagnostic and therapy
1017 systems. As the usage of the product and clinical screening usually need production at industrial
1018 scales, it is completely disparate from the laboratory scale. It is therefore extremely essential to

advance several innovative and simplified approaches for scale-up. Some of these restrictions and challenges can be overcome through using low cost sources of silica and organic agents needed for modification, decreased production steps, and improved safety caution through forming potential hazard controls. Besides, the protocols of fabrication, surface modifications, morphological alterations, and parameters of loading can make bring about variances in the biosafety consideration. Furthermore, controlled degradability of the last progressive MSN composites should be examined as a vital precondition for their usage in biomedical applications as the non-degradable manufacture can pose prolonged accumulation caused biosafety risks. Additionally, the ultimate elimination and degradability of their progressive prototypes solely relied on the clearance and biodistribution which can be influenced *via* the surface charge. Through modification, ligands that are sensitive to just one or two external stimuli such as magnetic field, temperature, US, and light or inner tissue/cell accessible signals, such as redox agents, enzyme, pH to the MSNs, can be employed as nanoplatforms for targeted delivery, localized and controlled release of numerous chemotherapeutics, enzyme, RNA and proteins. The anticancer properties of the prepared materials are expressively higher than that of free anti-tumoral. MSNs are generally used as a delivery reagent for the treatment of cancer and are delivered in most cases by the simple diffusion of cargos from the mesoporous to the surrounding medium. This significantly leads to a sustained delivery profile and improved cancer therapy. MSNs may therefore have novel applications in the commercial applications of nanomedicines. To aid this aim, clinical and pre-clinical trial examinations and laboratory designs should endeavor to probe and study the various variables in diagnosis and therapeutic applications in the future.

Declaration of competing interest

The authors declare no conflict of interest.

Authors contribution: Fatemeh Ahmadi, Arezoo Sodagar-Taleghani, Pedram Ebrahimnejad: Wrote and revised the manuscript. Seyyed Pouya Hadipour Moghaddam, Farzam Ebrahimnejad: Co-wrote the manuscript. Kofi Asare-Addo: reviewed and edited the manuscript. Ali Nokhodchi: revised the manuscript and supervised the research.

References

Ahn, B., Park, J., Singha, K., Park, H., Kim, W.J., 2013. Mesoporous silica nanoparticle-based cisplatin prodrug delivery and anticancer effect under reductive cellular environment. J Mater Chem B 1, 2829-2836.

Ahuja, G., Pathak, K., 2009. Porous carriers for controlled/modulated drug delivery. Indian J Pharm Sci 71, 599-607.

Alexis, F., Rhee, J.-W., Richie, J.P., Radovic-Moreno, A.F., Langer, R., Farokhzad, O.C., 2008. New frontiers in nanotechnology for cancer treatment, Urologic Oncology: Seminars and Original Investigations. Elsevier, pp. 74-85.

Amin, M.U., Ali, S., Tariq, I., Ali, M.Y., Pinnapreddy, S.R., Preis, E., Wölk, C., Harvey, R.D., Hause, G., Brüßler, J., Bakowsky, U., 2021. Ultrasound-responsive smart drug delivery system of lipid coated mesoporous silica nanoparticles. Pharmaceutics 13, 1-20.

Asefa, T., Tao, Z., 2012. Biocompatibility of mesoporous silica nanoparticles. Chem Res Toxicol 25, 2265-2284.

Avedian, N., Zaaeri, F., Daryasari, M.P., Javar, H.A., Khoobi, M., 2018. pH-sensitive biocompatible mesoporous magnetic nanoparticles labeled with folic acid as an efficient carrier for controlled anticancer drug delivery. J Drug Deliv Sci Technol 44, 323-332.

Aznar, E., Coll, C., Marcos, M.D., Martínez-Máñez, R., Sancenon, F., Soto, J., Amoros, P., Cano, J., Ruiz, E., 2009. Borate-driven gatelike scaffolding using mesoporous materials functionalised with saccharides. Chem Eur J 15, 6877-6888.

Bae, K.H., Chung, H.J., Park, T.G., 2011. Nanomaterials for cancer therapy and imaging. Mol Cells 31, 295-302.

Baeza, A., Guisasola, E., Ruiz-Hernandez, E., Vallet-Regí, M., 2012. Magnetically triggered multidrug release by hybrid mesoporous silica nanoparticles. Chem Mater 24, 517-524.

Baeza, A., Vallet-Regí, M., 2020. Mesoporous silica nanoparticles as theranostic antitumoral nanomedicines. Pharmaceutics 12, 1-16.

Baskar, R., Lee, K.A., Yeo, R., Yeoh, K.-W., 2012. Cancer and radiation therapy: current advances and future directions. Int J Med Sci 9, 193-199.

Bertrand, N., Wu, J., Xu, X., Kamaly, N., Farokhzad, O.C., 2014. Cancer nanotechnology: the impact of passive and active targeting in the era of modern cancer biology. Adv Drug Deliv Rev 66, 2-25.

Bharti, C., Nagaich, U., Pal, A.K., Gulati, N., 2015. Mesoporous silica nanoparticles in target drug delivery system: A review. Int J pharm investig 5, 124-133.

Biswas, N., 2017. Modified mesoporous silica nanoparticles for enhancing oral bioavailability and antihypertensive activity of poorly water soluble valsartan. Eur J Pharm Sci 99, 152-160.

Brinker, C.J., Carnes, E.C., Ashley, C.E., Willman, C.L., 2017. Porous nanoparticle-supported lipid bilayers (protocells) for targeted delivery and methods of using same. US20150272885A1.
Bukowski, K., Kciuk, M., Kontek, R., 2020. Mechanisms of multidrug resistance in cancer
Casasús, R., Marcos, M.D., Martínez-Máñez, R., Ros-Lis, J.V., Soto, J., Villaescusa, L.A., Amorós, P., Beltrán, D., Guillem, C., Latorre, J., 2004. Toward the development of ionically controlled nanoscopic molecular gates. J Am Chem Soc 126, 8612-8613.
Cauda, V., Argyo, C., Bein, T., 2010a. Impact of different PEGylation patterns on the long-term bio-stability of colloidal mesoporous silica nanoparticles. J Mater Chem 20, 8693-8699.
Cauda, V., Schlossbauer, A., Bein, T., 2010b. Bio-degradation study of colloidal mesoporous silica nanoparticles: Effect of surface functionalization with organo-silanes and poly (ethylene glycol). Microporous Mesoporous Mater 132, 60-71.
Chakravarty, R., Goel, S., Hong, H., Chen, F., Valdovinos, H.F., Hernandez, R., Barnhart, T.E., Cai, W., 2015. Hollow mesoporous silica nanoparticles for tumor vasculature targeting and PET image-guided drug delivery. Nanomedicine 10, 1233-1246.
Chang, D., Gao, Y., Wang, L., Liu, G., Chen, Y., Wang, T., Tao, W., Mei, L., Huang, L., Zeng, X., 2016. Polydopamine-based surface modification of mesoporous silica nanoparticles as pH-sensitive drug delivery vehicles for cancer therapy. J colloid interface sci 463, 279-287.
Chen, F., Goel, S., Valdovinos, H.F., Luo, H., Hernandez, R., Barnhart, T.E., Cai, W., 2015a. In vivo integrity and biological fate of chelator-free zirconium-89-labeled mesoporous silica nanoparticles. ACS Nano 9, 7950-7959.
Chen, F., Hong, H., Shi, S., Goel, S., Valdovinos, H.F., Hernandez, R., Theuer, C.P., Barnhart, T.E., Cai, W., 2014a. Engineering of hollow mesoporous silica nanoparticles for remarkably enhanced tumor active targeting efficacy. Sci Rep 4, 1-10.
Chen, F., Nayak, T.R., Goel, S., Valdovinos, H.F., Hong, H., Theuer, C.P., Barnhart, T.E., Cai, W., 2014b. In vivo tumor vasculature targeted PET/NIRF imaging with TRC105 (Fab)-conjugated, dual-labeled mesoporous silica nanoparticles. Mol Pharmaceutics 11, 4007-4014.
Chen, G., Teng, Z., Su, X., Liu, Y., Lu, G., 2015b. Unique biological degradation behavior of Stöber mesoporous silica nanoparticles from their interiors to their exteriors. J Biomed Nanotechnol 11, 722-729.
Chen, P.-J., Hu, S.-H., Hsiao, C.-S., Chen, Y.-Y., Liu, D.-M., Chen, S.-Y., 2011. Multifunctional magnetically removable nanogated lids of Fe3O4–capped mesoporous silica nanoparticles for intracellular controlled release and MR imaging. J Mater Chem 21, 2535-2543.
Chen, Y., Chen, H., Guo, L., He, Q., Chen, F., Zhou, J., Feng, J., Shi, J., 2010. ACS Nano 2010, 4, 529-539; b) Y. Chen, HR Chen, DP Zeng, YB Tian, F. Chen, JW Feng, JL Shi, ACS Nano 4, 6001-6013.
Chen, Y., Gu, H., Zhang, D.S.-Z., Li, F., Liu, T., Xia, W., 2014c. Highly effective inhibition of lung cancer growth and metastasis by systemic delivery of siRNA via multimodal mesoporous silica-based nanocarrier. Biomaterials 35, 10058-10069.
Chen, Y., Meng, Q., Wu, M., Wang, S., Xu, P., Chen, H., Li, Y., Zhang, L., Wang, L., Shi, J., 2014d. Hollow mesoporous organosilica nanoparticles: a generic intelligent framework-hybridization approach for biomedicine. J Am Chem Soc 136, 16326-16334.
Cheng, S.-H., Liao, W.-N., Chen, L.-M., Lee, C.-H., 2011. pH-controllable release using functionalized mesoporous silica nanoparticles as an oral drug delivery system. J Mater Chem 21, 7130-7137.
Cheng, W., Liang, C., Xu, L., Liu, G., Gao, N., Tao, W., Luo, L., Zuo, Y., Wang, X., Zhang, X., 2017. TPGS-functionalized polydopamine-modified mesoporous silica as drug nanocarriers for enhanced lung cancer chemotherapy against multidrug resistance. Small 13, 1700623.
Cheng, Y.-J., Luo, G.-F., Zhu, J.-Y., Xu, X.-D., Zeng, X., Cheng, D.-B., Li, Y.-M., Wu, Y., Zhang, X.-Z., Zhuo, R.-X., 2015. Enzyme-induced and tumor-targeted drug delivery system based on multifunctional mesoporous silica nanoparticles. ACS Appl Mater Interfaces 7, 9078-9087.

Choi, J.Y., Ramasamy, T., Kim, S.Y., Kim, J., Ku, S.K., Youn, Y.S., Kim, J.-R., Jeong, J.-H., Choi, H.-G., Yong, C.S., 2016. PEGylated lipid bilayer-supported mesoporous silica nanoparticle composite for synergistic co-delivery of axitinib and celastrol in multi-targeted cancer therapy. Acta Biomater

Climent, E., Bernardos, A., Martinez-Manez, R., Maquieira, A., Marcos, M.D., Pastor-Navarro, N., Puchades, R., Sancenón, F., Soto, J., Amorós, P., 2009. Controlled delivery systems using antibody-capped mesoporous nanocontainers. J Am Chem Soc 131, 14075-14080.
Colilla, M., González, B., Vallet-Regí, M., 2013. Mesoporous silica nanoparticles for the design of smart delivery nanodevices. Biomater Sci 1, 114-134.
Croissant, J., Chaix, A., Mongin, O., Wang, M., Clément, S., Raehm, L., Durand, J.O., Hugues, V., Blanchard-Desce, M., Maynadier, M., 2014. Two-Photon-Triggered Drug Delivery via Fluorescent Nanovalves. Small 10, 1752-1755.
Croissant, J.G., Fatieiev, Y., Almalik, A., Khashab, N.M., 2018. Mesoporous silica and organosilica nanoparticles: physical chemistry, biosafety, delivery strategies, and biomedical applications. Adv Healthcare Mater 7, 1700831.
Croissant, J.G., Fatieiev, Y., Khashab, N.M., 2017. Degradability and clearance of silicon, organosilica, silsesquioxane, silica mixed oxide, and mesoporous silica nanoparticles. Adv Mater 29, 1604634.
Cui, Y., Xu, Q., Chow, P.K.-H., Wang, D., Wang, C.-H., 2013. Transferrin-conjugated magnetic silica PLGA nanoparticles loaded with doxorubicin and paclitaxel for brain glioma treatment. Biomaterials 34, 8511-8520.
Dai, L., Li, J., Zhang, B., Liu, J., Luo, Z., Cai, K., 2014. Redox-responsive nanocarrier based on heparin end-capped mesoporous silica nanoparticles for targeted tumor therapy in vitro and in vivo. Langmuir 30, 7867-7877.
Dargaville, T.R., Farrugia, B.L., Broadbent, J.A., Pace, S., Upton, Z., Voelcker, N.H., 2013. Sensors and imaging for wound healing: a review. Biosens Bioelectron 41, 30-42.
Das, D.B., Mabrouk, M., Beherei, H.H., Arthanareeswaran, G., 2020. Pharmaceutical particulates and membranes for the delivery of drugs and bioactive molecules. Pharmaceutics 12, 1-4.
de Oliveira Freitas, L.B., de Melo Corgosinho, L., Faria, J.A.Q.A., dos Santos, V.M., Resende, J.M., Leal, A.S., Gomes, D.A., de Sousa, E.M.B., 2017. Multifunctional mesoporous silica nanoparticles for cancer-targeted, controlled drug delivery and imaging. Microporous Mesoporous Mater 242, 271-283.
Deng, Z., Zhen, Z., Hu, X., Wu, S., Xu, Z., Chu, P.K., 2011. Hollow chitosan–silica nanospheres as pH-sensitive targeted delivery carriers in breast cancer therapy. Biomaterials 32, 4976-4986.
DenizáYilmaz, M., FraseráStoddart, J., 2015. Esterase-and pH-responsive poly (β-amino ester)-capped mesoporous silica nanoparticles for drug delivery. Nanoscale 7, 7178-7183.
Deodhar, G.V., Adams, M.L., Trewyn, B.G., 2017. Controlled release and intracellular protein delivery from mesoporous silica nanoparticles. Biotechnol J 12, 1600408.
Doadrio, J.C., Sousa, E.M., Izquierdo-Barba, I., Doadrio, A.L., Perez-Pariente, J., Vallet-Regí, M., 2006. Functionalization of mesoporous materials with long alkyl chains as a strategy for controlling drug delivery pattern. J Mater Chem 16, 462-466.
dos Apostolos, R.C., Andrade, G.F., da Silva, W.M., de Assis Gomes, D., de Miranda, M.C., de Sousa, E.M., 2019. Hybrid polymeric systems of mesoporous silica/hydroxyapatite nanoparticles applied as antitumor drug delivery platform. Int J Appl Ceram Technol 16, 1836-1849.
Du, J., Lane, L.A., Nie, S., 2015. Stimuli-responsive nanoparticles for targeting the tumor microenvironment. J Control Release 219, 205-214.
Duo, Y., Yang, M., Du, Z., Feng, C., Xing, C., Wu, Y., Xie, Z., Zhang, F., Huang, L., Zeng, X., 2018. CX-5461-loaded nucleolus-targeting nanoplatform for cancer therapy through induction of pro-death autophagy. Acta biomater 79, 317-330.
Ebrahimnejad, P., Taleghani, A.S., Asare-Addo, K., Nokhodchi, A., 2022. An updated review of folate-functionalized nanocarriers: a promising ligand in cancer. Drug Discov Today 27, 471-489.

Egger, S.M., Hurley, K.R., Datt, A., Swindlehurst, G., Haynes, C.L., 2015. Ultraporous mesostructured silica nanoparticles. Chem Mater 27, 3193-3196.
Fadeel, B., Garcia-Bennett, A.E., 2010. Better safe than sorry: understanding the toxicological properties
362-374.
Famta, P., Shah, S., Chatterjee, E., Singh, H., Dey, B., Guru, S.K., Singh, S.B., Srivastava, S., 2021. Exploring new Horizons in overcoming P-glycoprotein-mediated multidrug-resistant breast cancer via nanoscale drug delivery platforms. Curr Res Pharmacol Drug Discov 6, 100054.
Fang, W., Yang, J., Gong, J., Zheng, N., 2012. Photo-and pH-triggered release of anticancer drugs from mesoporous silica-coated Pd@ Ag nanoparticles. Adv Funct Mater 22, 842-848.
Farjadian, F., Roointan, A., Mohammadi-Samani, S., Hosseini, M., 2019. Mesoporous silica nanoparticles: synthesis, pharmaceutical applications, biodistribution, and biosafety assessment. Chem Eng J 359, 684-705.
Feng, W., Nie, W., He, C., Zhou, X., Chen, L., Qiu, K., Wang, W., Yin, Z., 2014. Effect of pH-responsive alginate/chitosan multilayers coating on delivery efficiency, cellular uptake and biodistribution of mesoporous silica nanoparticles based nanocarriers. ACS appl Mater Interfaces 6, 8447-8460.
Feng, Y., Li, N.-x., Yin, H.-l., Chen, T.-y., Yang, Q., Wu, M., 2018. Thermo-and pH-responsive, lipid-coated, mesoporous silica nanoparticle-based dual drug delivery system to improve the antitumor effect of hydrophobic drugs. Mol Pharmaceutics 16, 422-436.
Ferris, D.P., Zhao, Y.-L., Khashab, N.M., Khatib, H.A., Stoddart, J.F., Zink, J.I., 2009. Light-operated mechanized nanoparticles. J Am Chem Soc 131, 1686-1688.
Finnie, K.S., Bartlett, J.R., Barbé, C.J., Kong, L., 2007. Formation of silica nanoparticles in microemulsions. Langmuir 23, 3017-3024.
Fox, M.E., Szoka, F.C., Fréchet, J.M., 2009. Soluble polymer carriers for the treatment of cancer: the importance of molecular architecture. Acc Chem Res 42, 1141-1151.
Fu, C., Liu, T., Li, L., Liu, H., Chen, D., Tang, F., 2013. The absorption, distribution, excretion and toxicity of mesoporous silica nanoparticles in mice following different exposure routes. Biomaterials 34, 2565-2575.
Ganguly, A., Ahmad, T., Ganguli, A.K., 2010. Silica mesostructures: Control of pore size and surface area using a surfactant-templated hydrothermal process. Langmuir 26, 14901-14908.
Gao, Q., Xie, W., Wang, Y., Wang, D., Guo, Z., Gao, F., Zhao, L., Cai, Q., 2018. A theranostic nanocomposite system based on radial mesoporous silica hybridized with Fe3O4 nanoparticles for targeted magnetic field responsive chemotherapy of breast cancer. RSC Adv 8, 4321-4328.
Gao, S., Zhang, L., Wang, G., Yang, K., Chen, M., Tian, R., Ma, Q., Zhu, L., 2016. Hybrid graphene/Au activatable theranostic agent for multimodalities imaging guided enhanced photothermal therapy. Biomaterials 79, 36-45.
Gao, Y., Gao, D., Shen, J., Wang, Q., 2020. A review of mesoporous silica nanoparticle delivery systems in chemo-based combination cancer therapies. Front Chem 8, 598722.
Gayam, S.R., Wu, S.-P., 2014. Redox responsive Pd (II) templated rotaxane nanovalve capped mesoporous silica nanoparticles: a folic acid mediated biocompatible cancer-targeted drug delivery system. J Mater Chem B 2, 7009-7016.
Giri, S., Trewyn, B.G., Stellmaker, M.P., Lin, V.S.Y., 2005. Stimuli-responsive controlled-release delivery system based on mesoporous silica nanorods capped with magnetic nanoparticles. Angew Chem Int Ed 44, 5038-5044.
Goel, S., England, C.G., Chen, F., Cai, W., 2017. Positron emission tomography and nanotechnology: A dynamic duo for cancer theranostics. Adv Drug Deliv Rev 113, 157-176.
Gonçalves, M., 2018. Sol-gel silica nanoparticles in medicine: A natural choice. Design, synthesis and products. Molecules 23, 1-26.
Gupta, A., Kushwaha, S.S., Mishra, A., 2020. A review on recent technologies and patents on silica nanoparticles for cancer Treatment and diagnosis. Recent Pat Drug Deliv Formul 14, 126-144.

Hadipour Moghaddam, S.P., Saikia, J., Yazdimamaghani, M., Ghandehari, H., 2017. Redox-responsive polysulfide-based biodegradable organosilica nanoparticles for delivery of bioactive agents. ACS Appl Mater Interfaces 9, 21133-21146.

Nanoscale 11, 799-819.
Hao, X., Hu, X., Zhang, C., Chen, S., Li, Z., Yang, X., Liu, H., Jia, G., Liu, D., Ge, K., 2016. Correction to hybrid mesoporous silica-based drug carrier nanostructures with improved degradability by hydroxyapatite. ACS Nano 10, 2983-2983.
Hasan-Nasab, B., Ebrahimnejad, P., Ebrahimi, P., Sharifi, F., Salili, M., Shahlaee, F., Nokhodchi, A., 2021. A promising targeting system to enrich irinotecan antitumor efficacy: Folic acid targeted nanoparticles. J Drug Deliv Sci Technol 63, 102543.
Hasanzadeh, M., Shadjou, N., de la Guardia, M., Eskandani, M., Sheikhzadeh, P., 2012. Mesoporous silica-based materials for use in biosensors. Trends Anal Chem 33, 117-129.
He, D., He, X., Wang, K., Chen, M., Cao, J., Zhao, Y., 2012. Reversible stimuli-responsive controlled release using mesoporous silica nanoparticles functionalized with a smart DNA molecule-gated switch. J Mater Chem 22, 14715-14721.
He, Q., Shi, J., 2014. MSN anti-cancer nanomedicines: chemotherapy enhancement, overcoming of drug resistance, and metastasis inhibition. Adv Mater 26, 391-411.
Heidari, R., Khosravian, P., Mirzaei, S.A., Elahian, F., 2021. siRNA delivery using intelligent chitosan-capped mesoporous silica nanoparticles for overcoming multidrug resistance in malignant carcinoma cells. Sci Rep 11, 1-14.
Hoare, T., Santamaria, J., Goya, G.F., Irusta, S., Lin, D., Lau, S., Padera, R., Langer, R., Kohane, D.S., 2009. A magnetically triggered composite membrane for on-demand drug delivery. Nano Lett 9, 3651-3657.
Huang, P., Chen, Y., Lin, H., Yu, L., Zhang, L., Wang, L., Zhu, Y., Shi, J., 2017. Molecularly organic/inorganic hybrid hollow mesoporous organosilica nanocapsules with tumor-specific biodegradability and enhanced chemotherapeutic functionality. Biomaterials 125, 23-37.
Huang, X., Li, L., Liu, T., Hao, N., Liu, H., Chen, D., Tang, F., 2011. The shape effect of mesoporous silica nanoparticles on biodistribution, clearance, and biocompatibility in vivo. ACS Nano 5, 5390-5399.
Huang, X., Teng, X., Chen, D., Tang, F., He, J., 2010. The effect of the shape of mesoporous silica nanoparticles on cellular uptake and cell function. Biomaterials 31, 438-448.
Hudson, S.P., Padera, R.F., Langer, R., Kohane, D.S., 2008. The biocompatibility of mesoporous silicates. Biomaterials 29, 4045-4055.
Hwang, A.A., Lu, J., Tamanoi, F., Zink, J.I., 2015. Functional nanovalves on protein-coated nanoparticles for in vitro and in vivo controlled drug delivery. Small 11, 319-328.
Jafari, M., Heidari, D., Ebrahimnejad, P., 2016. Synthesizing and characterizing functionalized short multiwall carbon nanotubes with folate, magnetite and polyethylene glycol as multi-targeted nanocarrier of anti-cancer drugs. Iranian journal of pharmaceutical research: IJPR 15, 449.
Jafari, S., Derakhshankhah, H., Alaei, L., Fattahi, A., Varnamkhasti, B.S., Saboury, A.A., Pharmacotherapy, 2019. Mesoporous silica nanoparticles for therapeutic/diagnostic applications. Biomed Pharmacother 109, 1100-1111.
Jakobsson, U., Mäkilä, E., Airaksinen, A.J., Alanen, O., Etilé, A., Köster, U., Ranjan, S., Salonen, J., Santos, H.A., Helariutta, K., 2019. Porous silicon as a platform for radiation theranostics together with a novel RIB-based radiolanthanoid. Contrast media & mol imaging 2019, 1-9.
Janjua, T.I., Cao, Y., Yu, C., Popat, A., 2021. Clinical translation of silica nanoparticles. Nat Rev Mater 6, 1072-1074.
Jeong, H.J., Yoo, R.J., Kim, J.K., Kim, M.H., Park, S.H., Kim, H., Lim, J.W., Do, S.H., Lee, K.C., Lee, Y.J., Kim, D.W., 2019. Macrophage cell tracking PET imaging using mesoporous silica nanoparticles via in vivo bioorthogonal F-18 labeling. Biomaterials 199, 32-39.

Jia, L., Li, Z., Shen, J., Zheng, D., Tian, X., Guo, H., Chang, P., 2015. Multifunctional mesoporous silica nanoparticles mediated co-delivery of paclitaxel and tetrandrine for overcoming multidrug resistance. Int J Pharm 489, 318-330.

evaluation of paclitaxel-loaded mesoporous silica nanoparticles with three pore sizes. Int J Pharm 445, 12-19.
Kammler, H.K., Beaucage, G., Mueller, R., Pratsinis, S.E., 2004. Structure of flame-made silica nanoparticles by ultra-small-angle X-ray scattering. Langmuir 20, 1915-1921.
Kankala, R.K., Han, Y.-H., Xia, H.-Y., Wang, S.-B., Chen, A.-Z., 2022. Nanoarchitectured prototypes of mesoporous silica nanoparticles for innovative biomedical applications. J Nanobiotechnology 20, 1-67.
Kankala, R.K., Han, Y.H., Na, J., Lee, C.H., Sun, Z., Wang, S.B., Kimura, T., Ok, Y.S., Yamauchi, Y., Chen, A.Z., Wu, K.C.W., 2020a. Nanoarchitectured structure and surface biofunctionality of mesoporous silica nanoparticles. Adv Mater 32, 1907035.
Kankala, R.K., Liu, C.-G., Chen, A.-Z., Wang, S.-B., Xu, P.-Y., Mende, L.K., Liu, C.-L., Lee, C.-H., Hu, Y.-F., 2017. Overcoming multidrug resistance through the synergistic effects of hierarchical pH-sensitive, ROS-generating nanoreactors. ACS Biomater Sci Eng 3, 2431-2442.
Kankala, R.K., Liu, C.-G., Yang, D.-Y., Wang, S.-B., Chen, A.-Z., 2020b. Ultrasmall platinum nanoparticles enable deep tumor penetration and synergistic therapeutic abilities through free radical species-assisted catalysis to combat cancer multidrug resistance. Chem Eng J 383, 123138.
Kankala, R.K., Wang, S.-B., Chen, A.-Z., 2020c. Nanoarchitecting hierarchical mesoporous siliceous frameworks: a new way forward. Iscience 23, 101687.
Kankala, R.K., Zhang, H., Liu, C.G., Kanubaddi, K.R., Lee, C.H., Wang, S.B., Cui, W., Santos, H.A., Lin, K., Chen, A.Z., 2019. Metal species–encapsulated mesoporous silica nanoparticles: current advancements and latest breakthroughs. Adv Funct Mater 29, 1902652.
Keerl, M., Smirnovas, V., Winter, R., Richtering, W., 2008. Copolymer microgels from mono-and disubstituted acrylamides: phase behavior and hydrogen bonds. Macromolecules 41, 6830-6836.
Kiessling, F., Fokong, S., Bzyl, J., Lederle, W., Palmowski, M., Lammers, T., 2014. Recent advances in molecular, multimodal and theranostic ultrasound imaging. Adv Drug Deliv Rev 72, 15-27.
Knežević, N.Ž, Mrđanović, J., Borišev, I., Milenković, S., Janaćković, Đ., Cunin, F., Djordjevic, A., 2016. Hydroxylated fullerene-capped, vinblastine-loaded folic acid-functionalized mesoporous silica nanoparticles for targeted anticancer therapy. RSC Adv 6, 7061-7065.
Kohane, D.S., Langer, R., 2010. Biocompatibility and drug delivery systems. Chem Sci 1, 441-446.
Kumar, B., Kulanthaivel, S., Mondal, A., Mishra, S., Banerjee, B., Bhaumik, A., Banerjee, I., Giri, S., 2017. Mesoporous silica nanoparticle based enzyme responsive system for colon specific drug delivery through guar gum capping. Colloids Surf B 150, 352-361.
Lai, C.-Y., Trewyn, B.G., Jeftinija, D.M., Jeftinija, K., Xu, S., Jeftinija, S., Lin, V.S.-Y., 2003. A mesoporous silica nanosphere-based carrier system with chemically removable CdS nanoparticle caps for stimuli-responsive controlled release of neurotransmitters and drug molecules. J Am Chem Soc 125, 4451-4459.
Lee, C.-H., Lin, T.-S., Mou, C.-Y., 2009. Mesoporous materials for encapsulating enzymes. Nano Today 4, 165-179.
Lee, J.E., Lee, N., Kim, H., Kim, J., Choi, S.H., Kim, J.H., Kim, T., Song, I.C., Park, S.P., Moon, W.K., 2010. Uniform mesoporous dye-doped silica nanoparticles decorated with multiple magnetite nanocrystals for simultaneous enhanced magnetic resonance imaging, fluorescence imaging, and drug delivery. J Am Chem Soc 132, 552-557.
Lee, S.-F., Zhu, X.-M., Wang, Y.-X.J., Xuan, S.-H., You, Q., Chan, W.-H., Wong, C.-H., Wang, F., Yu, J.C., Cheng, C.H., 2013. Ultrasound, pH, and magnetically responsive crown-ether-coated core/shell nanoparticles as drug encapsulation and release systems. ACS appl Mater Interfaces 5, 1566-1574.

Lei, Q., Guo, J., Noureddine, A., Wang, A., Wuttke, S., Brinker, C.J., Zhu, W., 2020. Sol–gel-based advanced porous silica materials for biomedical applications. Adv Funct Mater 30, 1909539.
Li, L., Liu, T., Fu, C., Tan, L., Meng, X., Liu, H., 2015a. Biodistribution, excretion, and toxicity of
1915-1924.
Li, M., Sun, J., Zhang, W., Zhao, Y., Zhang, S., Zhang, S., 2021. Drug delivery systems based on CD44-targeted glycosaminoglycans for cancer therapy. Carbohydr Polym 251, 117103.
Li, T., Shen, X., Geng, Y., Chen, Z., Li, L., Li, S., Yang, H., Wu, C., Zeng, H., Liu, Y., 2016. Folate-functionalized magnetic-mesoporous silica nanoparticles for drug/gene codelivery to potentiate the antitumor efficacy. ACS Appl Mater Interfaces 8, 13748-13758.
Li, T., Shi, S., Goel, S., Shen, X., Xie, X., Chen, Z., Zhang, H., Li, S., Qin, X., Yang, H., Wu, C., Liu, Y., 2019. Recent advancements in mesoporous silica nanoparticles towards therapeutic applications for cancer. Acta Biomater 89, 1-13.
Li, W.-P., Liao, P.-Y., Su, C.-H., Yeh, C.-S., 2014. Formation of oligonucleotide-gated silica shell-coated Fe3O4-Au core–shell nanotrisoctahedra for magnetically targeted and near-infrared light-responsive theranostic platform. J Am Chem Soc 136, 10062-10075.
Li, X., Sun, W., Zhang, Z., Kang, Y., Fan, J., Peng, X., 2020. Red Light-Triggered Polyethylene Glycol Deshielding from Photolabile Cyanine-Modified Mesoporous Silica Nanoparticles for On-Demand Drug Release. ACS Appl Bio Mater 3, 8084-8093.
Li, X., Xing, L., Hu, Y., Xiong, Z., Wang, R., Xu, X., Du, L., Shen, M., Shi, X., 2017a. An RGD-modified hollow silica@ Au core/shell nanoplatform for tumor combination therapy. Acta biomater 62, 273-283.
Li, Z.-Y., Hu, J.-J., Xu, Q., Chen, S., Jia, H.-Z., Sun, Y.-X., Zhuo, R.-X., Zhang, X.-Z., 2015b. A redox-responsive drug delivery system based on RGD containing peptide-capped mesoporous silica nanoparticles. J Mater Chem B 3, 39-44.
Li, Z., Tan, S., Li, S., Shen, Q., Wang, K., 2017b. Cancer drug delivery in the nano era: An overview and perspectives. Oncol Rep 38, 611-624.
Liberti, M.V., Locasale, J.W., 2016. The Warburg effect: how does it benefit cancer cells? Trends Biochem Sci 41, 211-218.
Lin, Q., Huang, Q., Li, C., Bao, C., Liu, Z., Li, F., Zhu, L., 2010. Anticancer drug release from a mesoporous silica based nanophotocage regulated by either a one-or two-photon process. J Am Chem Soc 132, 10645-10647.
Lin, Y.-S., Haynes, C.L., 2010. Impacts of mesoporous silica nanoparticle size, pore ordering, and pore integrity on hemolytic activity. J Am Chem Soc 132, 4834-4842.
Liong, M., Lu, J., Kovochich, M., Xia, T., Ruehm, S.G., Nel, A.E., Tamanoi, F., Zink, J.I., 2008. Multifunctional inorganic nanoparticles for imaging, targeting, and drug delivery. ACS Nano 2, 889-896.
Liu, H., Chen, D., Li, L., Liu, T., Tan, L., Wu, X., Tang, F., 2011a. Multifunctional gold nanoshells on silica nanorattles: a platform for the combination of photothermal therapy and chemotherapy with low systemic toxicity. Angew Chem Int Ed 50, 891-895.
Liu, H.M., Wu, S.H., Lu, C.W., Yao, M., Hsiao, J.K., Hung, Y., Lin, Y.S., Mou, C.Y., Yang, C.S., Huang, D.M., Chen, Y.C., 2008. Mesoporous silica nanoparticles improve magnetic labeling efficiency in human stem cells. Small 4, 619-626.
Liu, J., Zhang, B., Luo, Z., Ding, X., Li, J., Dai, L., Zhou, J., Zhao, X., Ye, J., Cai, K., 2015a. Enzyme responsive mesoporous silica nanoparticles for targeted tumor therapy in vitro and in vivo. Nanoscale 7, 3614-3626.
Liu, T.-P., Wu, S.-H., Chen, Y.-P., Chou, C.-M., Chen, C.-T., 2015b. Biosafety evaluations of well-dispersed mesoporous silica nanoparticles: towards in vivo-relevant conditions. Nanoscale 7, 6471-6480.

Liu, T., Li, L., Teng, X., Huang, X., Liu, H., Chen, D., Ren, J., He, J., Tang, F., 2011b. Single and repeated dose toxicity of mesoporous hollow silica nanoparticles in intravenously exposed mice. Biomaterials 32, 1657-1668.

generation of O2 bubbles for in situ ultrasound-guided high intensity focused ultrasound ablation. ACS Nano 11, 9093-9102.
Lu, J., Choi, E., Tamanoi, F., Zink, J.I., 2008. Light-activated nanoimpeller-controlled drug release in cancer cells. Small 4, 421-426.
Lu, J., Liong, M., Li, Z., Zink, J.I., Tamanoi, F., 2010. Biocompatibility, biodistribution, and drug-delivery efficiency of mesoporous silica nanoparticles for cancer therapy in animals. Small 6, 1794-1805.
Lu, J., Liong, M., Zink, J.I., Tamanoi, F., 2007. Mesoporous silica nanoparticles as a delivery system for hydrophobic anticancer drugs. small 3, 1341-1346.
Luo, G.-F., Chen, W.-H., Liu, Y., Lei, Q., Zhuo, R.-X., Zhang, X.-Z., 2014. Multifunctional enveloped mesoporous silica nanoparticles for subcellular co-delivery of drug and therapeutic peptide. Sci Rep 4, 6064.
Luo, Z., Cai, K., Hu, Y., Zhao, L., Liu, P., Duan, L., Yang, W., 2011. Mesoporous silica nanoparticles end-capped with collagen: redox-responsive nanoreservoirs for targeted drug delivery. Angew Chem Int Ed 50, 640-643.
M Rosenholm, J., Sahlgren, C., Lindén, M., 2011. Multifunctional mesoporous silica nanoparticles for combined therapeutic, diagnostic and targeted action in cancer treatment. Curr drug targets 12, 1166-1186.
Ma, M., Chen, H., Chen, Y., Zhang, K., Wang, X., Cui, X., Shi, J., 2012. Hyaluronic acid-conjugated mesoporous silica nanoparticles: excellent colloidal dispersity in physiological fluids and targeting efficacy. J Mater Chem 22, 5615-5621.
Ma, X., Teh, C., Zhang, Q., Borah, P., Choong, C., Korzh, V., Zhao, Y., 2014. Redox-responsive mesoporous silica nanoparticles: a physiologically sensitive codelivery vehicle for siRNA and doxorubicin. Antioxid redox signaling 21, 707-722.
Mal, N.K., Fujiwara, M., Tanaka, Y., 2003. Photocontrolled reversible release of guest molecules from coumarin-modified mesoporous silica. Nature 421, 350-353.
Martelli, G., Zope, H.R., Capell, M.B., Kros, A., 2013. Coiled-coil peptide motifs as thermoresponsive valves for mesoporous silica nanoparticles. Chem commun 49, 9932-9934.
Martinez, H.P., Kono, Y., Blair, S.L., Sandoval, S., Wang-Rodriguez, J., Mattrey, R.F., Kummel, A.C., Trogler, W.C., 2010. Hard shell gas-filled contrast enhancement particles for colour Doppler ultrasound imaging of tumors. MedChemComm 1, 266-270.
Matapurkar, A., Lazebnik, Y., 2006. Requirement of cytochrome c for apoptosis in human cells. Cell Death & Differ 13, 2062-2067.
Maurer-Jones, M.A., Lin, Y.-S., Haynes, C.L., 2010. Functional assessment of metal oxide nanoparticle toxicity in immune cells. ACS Nano 4, 3363-3373.
Mehmood, A., Ghafar, H., Yaqoob, S., Gohar, U.F., Ahmad, B., 2017. Mesoporous silica nanoparticles: a review. J Dev Drugs 6, 1-14.
Meng, H., Liong, M., Xia, T., Li, Z., Ji, Z., Zink, J.I., Nel, A.E., 2010. Engineered design of mesoporous silica nanoparticles to deliver doxorubicin and P-glycoprotein siRNA to overcome drug resistance in a cancer cell line. ACS Nano 4, 4539-4550.
Meng, H., Wang, M., Liu, H., Liu, X., Situ, A., Wu, B., Ji, Z., Chang, C.H., Nel, A.E., 2015. Use of a lipid-coated mesoporous silica nanoparticle platform for synergistic gemcitabine and paclitaxel delivery to human pancreatic cancer in mice. ACS nano 9, 3540-3557.
Miller, L., Winter, G., Baur, B., Witulla, B., Solbach, C., Reske, S., Lindén, M., 2014. Synthesis, characterization, and biodistribution of multiple 89 Zr-labeled pore-expanded mesoporous silica nanoparticles for PET. Nanoscale 6, 4928-4935.

Mir, M., Ebrahimnejad, P., 2014. Preparation and characterization of bifunctional nanoparticles of vitamin E TPGS-emulsified PLGA-PEG-FOL containing deferasirox. Nanosci nanotechnol-asia 4, 80-87.

Funct Mater 17, 605-612.
Moghaddam, S.P.H., Mohammadpour, R., Ghandehari, H., 2019. In vitro and in vivo evaluation of degradation, toxicity, biodistribution, and clearance of silica nanoparticles as a function of size, porosity, density, and composition. J Control Release 311, 1-15.
Moghaddam, S.P.H., Yazdimamaghani, M., Ghandehari, H., 2018. Glutathione-sensitive hollow mesoporous silica nanoparticles for controlled drug delivery. J Control Release 282, 62-75.
Mohammadpour, R., Cheney, D.L., Grunberger, J.W., Yazdimamaghani, M., Jedrzkiewicz, J., Isaacson, K.J., Dobrovolskaia, M.A., Ghandehari, H., 2020. One-year chronic toxicity evaluation of single dose intravenously administered silica nanoparticles in mice and their Ex vivo human hemocompatibility. J Control Release 324, 471-481.
Mohammady, H., Dinarvand, R., Esfandyari Manesh, M., Ebrahimnejad, P., 2016. Encapsulation of irinotecan in polymeric nanoparticles: Characterization, release kinetic and cytotoxicity evaluation. Nanomed J 3, 159-168.
Möller, K., Müller, K., Engelke, H., Bräuchle, C., Wagner, E., Bein, T., 2016. Highly efficient siRNA delivery from core–shell mesoporous silica nanoparticles with multifunctional polymer caps. Nanoscale 8, 4007-4019.
Monem, A.S., Elbialy, N., Mohamed, N., 2014. Mesoporous silica coated gold nanorods loaded doxorubicin for combined chemo–photothermal therapy. Int J Pharm 470, 1-7.
Mu, S., Liu, Y., Wang, T., Zhang, J., Jiang, D., Yu, X., Zhang, N., 2017. Unsaturated nitrogen-rich polymer poly (l-histidine) gated reversibly switchable mesoporous silica nanoparticles using "graft to" strategy for drug controlled release. Acta biomater 63, 150-162.
Murugan, B., Sagadevan, S., Fatimah, I., Oh, W.-C., Hossain, M.A.M., Johan, M.R., 2021. Smart stimuli-responsive nanocarriers for the cancer therapy–nanomedicine. Nanotechnol Rev 10, 933-953.
Nadrah, P., Maver, U., Jemec, A., Tišler, T., Bele, M., Dražić, G., Benčina, M., Pintar, A., Planinšek, O., Gaberšček, M., 2013a. Hindered disulfide bonds to regulate release rate of model drug from mesoporous silica. ACS Appl Mater Interfaces 5, 3908-3915.
Nadrah, P., Porta, F., Planinšek, O., Kros, A., Gaberšček, M., 2013b. Poly (propylene imine) dendrimer caps on mesoporous silica nanoparticles for redox-responsive release: smaller is better. Phys Chem Chem Physi 15, 10740-10748.
Nagase, K., Kobayashi, J., Kikuchi, A., Akiyama, Y., Kanazawa, H., Okano, T., 2007. Interfacial property modulation of thermoresponsive polymer brush surfaces and their interaction with biomolecules. Langmuir 23, 9409-9415.
Narayan, R., Nayak, U.Y., Raichur, A.M., Garg, S., 2018. Mesoporous silica nanoparticles: A comprehensive review on synthesis and recent advances. Pharmaceutics 10, 118.
Nash, T., Allison, A., Harington, J., 1966. Physico-chemical properties of silica in relation to its toxicity. Nature 210, 259-261.
Natarajan, S.K., Selvaraj, S., 2014. Mesoporous silica nanoparticles: importance of surface modifications and its role in drug delivery. RSC Adv 4, 14328-14334.
Naz, S., Wang, M., Han, Y., Hu, B., Teng, L., Zhou, J., Zhang, H., Chen, J., 2019. Enzyme-responsive mesoporous silica nanoparticles for tumor cells and mitochondria multistage-targeted drug delivery. Int J Nanomed 14, 2533.
Nel, A.E., Mädler, L., Velegol, D., Xia, T., Hoek, E., Somasundaran, P., Klaessig, F., Castranova, V., Thompson, M., 2009. Understanding biophysicochemical interactions at the nano–bio interface. Nat Mater 8, 543-557.
Nel, A.E., Zink, J.I., Meng, H., 2016. Lipid bilayer coated mesoporous silica nanoparticles with a high loading capacity for one or more anticancer agents. US20160008283A1.

Ni, D., Bu, W., Ehlerding, E.B., Cai, W., Shi, J., 2017. Engineering of inorganic nanoparticles as magnetic resonance imaging contrast agents. Chem Soc Rev 46, 7438-7468.
Niedermayer, S., Weiss, V., Herrmann, A., Schmidt, A., Datz, S., Müller, K., Wagner, E., Bein, T., responsive targeted drug delivery. Nanoscale 7, 7953-7964.
Niemelä, E., Desai, D., Nkizinkiko, Y., Eriksson, J.E., Rosenholm, J.M., 2015. Sugar-decorated mesoporous silica nanoparticles as delivery vehicles for the poorly soluble drug celastrol enables targeted induction of apoptosis in cancer cells. Eur J Pharm Biopharm 96, 11-21.
Niu, D., Ma, Z., Li, Y., Shi, J., 2010. Synthesis of core− shell structured dual-mesoporous silica spheres with tunable pore size and controllable shell thickness. J Am Chem Soc 132, 15144-15147.
Overall, C.M., Kleifeld, O., 2006. Validating matrix metalloproteinases as drug targets and anti-targets for cancer therapy. Nat Rev Cancer 6, 227-239.
Pan, G., Jia, T.-t., Huang, Q.-x., Qiu, Y.-y., Xu, J., Yin, P.-h., Liu, T., 2017. Mesoporous silica nanoparticles (MSNs)-based organic/inorganic hybrid nanocarriers loading 5-Fluorouracil for the treatment of colon cancer with improved anticancer efficacy. Colloids Surf B 159, 375-385.
Pan, L., He, Q., Liu, J., Chen, Y., Ma, M., Zhang, L., Shi, J., 2012. Nuclear-targeted drug delivery of TAT peptide-conjugated monodisperse mesoporous silica nanoparticles. J Am Chem Soc 134, 5722-5725.
Pan, L., Liu, J., He, Q., Shi, J., 2014. MSN-mediated sequential vascular-to-cell nuclear-targeted drug delivery for efficient tumor regression. Adv Mater 26, 6742-6748.
Pan, L., Liu, J., He, Q., Wang, L., Shi, J., 2013. Overcoming multidrug resistance of cancer cells by direct intranuclear drug delivery using TAT-conjugated mesoporous silica nanoparticles. Biomaterials 34, 2719-2730.
Paris, J.L., Cabañas, M.V., Manzano, M., Vallet-Regí, M., 2015. Polymer-grafted mesoporous silica nanoparticles as ultrasound-responsive drug carriers. ACS Nano 9, 11023-11033.
Park, S., Park, H., Jeong, S., Yi, B.G., Park, K., Key, J., 2019. Hyaluronic acid-conjugated mesoporous silica nanoparticles loaded with dual anticancer agents for chemophotodynamic cancer therapy. Journal of Nanomaterials 2019.
Patel, A.C., Li, S., Yuan, J.-M., Wei, Y., 2006. In situ encapsulation of horseradish peroxidase in electrospun porous silica fibers for potential biosensor applications. Nano lett 6, 1042-1046.
Peng, X., Lin, G., Zeng, Y., Lei, Z., Liu, G., Biotechnology, 2021. Mesoporous Silica Nanoparticle-Based Imaging Agents for Hepatocellular Carcinoma Detection. Front Bioeng Biotechnol 9, 749381.
Rahikkala, A., Pereira, S.A., Figueiredo, P., Passos, M.L., Araujo, A.R., Saraiva, M.L.M.M., Santos, H.A., 2018. Mesoporous silica nanoparticles for targeted and stimuli-responsive delivery of chemotherapeutics: A review. Adv Biosyst 2, 1800020.
Rahman, I.A., Padavettan, V., 2012. Synthesis of silica nanoparticles by sol-gel: size-dependent properties, surface modification, and applications in silica-polymer nanocomposites—a review. J Nanomater 2012, 1-15.
Raj, S., Khurana, S., Choudhari, R., Kesari, K.K., Kamal, M.A., Garg, N., Ruokolainen, J., Das, B.C., Kumar, D., 2021. Specific targeting cancer cells with nanoparticles and drug delivery in cancer therapy, Seminars in Cancer Biology. Elsevier, pp. 166-177.
Rosenblum, D., Joshi, N., Tao, W., Karp, J.M., Peer, D.J.N.c., 2018. Progress and challenges towards targeted delivery of cancer therapeutics. 9, 1-12.
Rosenholm, J.M., Meinander, A., Peuhu, E., Niemi, R., Eriksson, J.E., Sahlgren, C., Lindén, M., 2009. Targeting of porous hybrid silica nanoparticles to cancer cells. ACS nano 3, 197-206.
Rosenholm, J.M., Peuhu, E., Bate-Eya, L.T., Eriksson, J.E., Sahlgren, C., Lindén, M., 2010. Cancer-cell-specific induction of apoptosis using mesoporous silica nanoparticles as drug-delivery vectors. Small 6, 1234-1241.

Sadeghi-Ghadi, Z., Ebrahimnejad, P., Talebpour Amiri, F., Nokhodchi, A., 2021. Improved oral delivery of quercetin with hyaluronic acid containing niosomes as a promising formulation. J Drug Targeting 29, 225-234.

vitro activity of curcumin and quercetin co-encapsulated in nanovesicles without hyaluronan against Aspergillus and Candida isolates. J Mycol Med 30, 101014.
Saint-Cricq, P., Deshayes, S., Zink, J., Kasko, A., 2015. Magnetic field activated drug delivery using thermodegradable azo-functionalised PEG-coated core–shell mesoporous silica nanoparticles. Nanoscale 7, 13168-13172.
Sanson, C., Diou, O., Thevenot, J., Ibarboure, E., Soum, A., Brûlet, A., Miraux, S., Thiaudière, E., Tan, S., Brisson, A., 2011. Doxorubicin loaded magnetic polymersomes: theranostic nanocarriers for MR imaging and magneto-chemotherapy. ACS Nano 5, 1122-1140.
Saroj, S., Rajput, S.J., 2018. Tailor-made pH-sensitive polyacrylic acid functionalized mesoporous silica nanoparticles for efficient and controlled delivery of anti-cancer drug Etoposide. Drug Deve Ind Pharm 44, 1198-1211.
Sasikala, A.R.K., Thomas, R.G., Unnithan, A.R., Saravanakumar, B., Jeong, Y.Y., Park, C.H., Kim, C.S., 2016. Multifunctional nanocarpets for cancer theranostics: remotely controlled graphene nanoheaters for thermo-chemosensitisation and magnetic resonance imaging. Sci Rep 6, 20543.
Schlossbauer, A., Kecht, J., Bein, T., 2009. Biotin–Avidin as a protease-responsive cap system for controlled guest release from colloidal mesoporous silica. Angew Chem Int Ed 48, 3092-3095.
Schlossbauer, A., Warncke, S., Gramlich, P.M., Kecht, J., Manetto, A., Carell, T., Bein, T., 2010. A programmable DNA-based molecular valve for colloidal mesoporous silica. Angew chem Int Ed 49, 4734-4737.
Serda, R.E., Meraz, I.M., Gu, J., Xia, X., Shen, H., Sun, T., Ferrari, M., 2015. Mesoporous silicon particles for the presentation of tumor antigens and adjuvant for anti-cancer immunity. US8926994B2.
Shao, D., Lu, M.-m., Zhao, Y.-w., Zhang, F., Tan, Y.-f., Zheng, X., Pan, Y., Xiao, X.-a., Wang, Z., Dong, W.-f., Li, J., 2017. The shape effect of magnetic mesoporous silica nanoparticles on endocytosis, biocompatibility and biodistribution. Acta Biomater 49, 531-540.
Sharifi, F., Jahangiri, M., Ebrahimnejad, P., 2021a. Synthesis of novel polymeric nanoparticles (methoxy-polyethylene glycol-chitosan/hyaluronic acid) containing 7-ethyl-10-hydroxycamptothecin for colon cancer therapy: in vitro, ex vivo and in vivo investigation. Artif Cells, Nanomed, Biotechnol 49, 367-380.
Sharifi, F., Jahangiri, M., Nazir, I., Asim, M.H., Ebrahimnejad, P., Hupfauf, A., Gust, R., Bernkop-Schnürch, A., 2021b. Zeta potential changing nanoemulsions based on a simple zwitterion. J Colloid Interface Sci 585, 126-137.
Shi, S., Chen, F., Cai, W., 2013. Biomedical applications of functionalized hollow mesoporous silica nanoparticles: focusing on molecular imaging. Nanomedicine 8, 2027-2039.
Singh, L.P., Bhattacharyya, S.K., Kumar, R., Mishra, G., Sharma, U., Singh, G., Ahalawat, S., 2014. Sol-Gel processing of silica nanoparticles and their applications. Adv Colloid Interface Sci 214, 17-37.
Sirsi, S.R., Borden, M.A., 2014. State-of-the-art materials for ultrasound-triggered drug delivery. Adv Drug Deliv Rev 72, 3-14.
Slowing, I., Trewyn, B.G., Lin, V.S.-Y., 2006. Effect of surface functionalization of MCM-41-type mesoporous silica nanoparticles on the endocytosis by human cancer cells. J Am Chem Soc 128, 14792-14793.
Slowing, I.I., Wu, C.W., Vivero-Escoto, J.L., Lin, V.S.Y., 2009. Mesoporous silica nanoparticles for reducing hemolytic activity towards mammalian red blood cells. Small 5, 57-62.
Smith, A.M., Duan, H., Mohs, A.M., Nie, S., 2008. Bioconjugated quantum dots for in vivo molecular and cellular imaging. Adv Drug Deliv Rev 60, 1226-1240.

Sodagar-Taleghani, A., Ebrahimnejad, P., Heidarinasab, A., Akbarzadeh, A., 2019. Sugar-conjugated dendritic mesoporous silica nanoparticles as pH-responsive nanocarriers for tumor targeting and controlled release of deferasirox. Mater Sci Eng C 98, 358-368.

controlled release of iron-chelating drug from the amino-terminated PAMAM/ordered mesoporous silica hybrid materials. J Drug Deliv Sci Technol 56, 101579.
Sodagar-Taleghani, A., Nakhjiri, A.T., Khakzad, M.J., Rezayat, S.M., Ebrahimnejad, P., Heydarinasab, A., Akbarzadeh, A., Marjani, A., 2021. Mesoporous silica nanoparticles as a versatile nanocarrier for cancer treatment: A review. J Mol Liq, 328, 115417.
Song, J.-T., Yang, X.-Q., Zhang, X.-S., Yan, D.-M., Wang, Z.-Y., Zhao, Y.-D., 2015. Facile synthesis of gold nanospheres modified by positively charged mesoporous silica, loaded with near-infrared fluorescent dye, for in vivo X-ray computed tomography and fluorescence dual mode imaging. ACS Appl Mater Interfaces 7, 17287-17297.
Souris, J.S., Lee, C.-H., Cheng, S.-H., Chen, C.-T., Yang, C.-S., Ja-an, A.H., Mou, C.-Y., Lo, L.-W., 2010. Surface charge-mediated rapid hepatobiliary excretion of mesoporous silica nanoparticles. Biomaterials 31, 5564-5574.
Srinivasarao, M., Low, P.S., 2017. Ligand-targeted drug delivery. Chem Rev 117, 12133-12164.
Subhan, M.A., Yalamarty, S.S.K., Filipczak, N., Parveen, F., Torchilin, V.P., 2021. Recent advances in tumor targeting via EPR effect for cancer treatment. J Pers Med 11, 1-27.
Sun, B., Zhen, X., Jiang, X., 2021. Development of mesoporous silica-based nanoprobes for optical bioimaging applications. Biomater Sci 9, 3603-3620.
Sun, J.T., Yu, Z.Q., Hong, C.Y., Pan, C.Y., 2012. Biocompatible zwitterionic sulfobetaine copolymer-coated mesoporous silica nanoparticles for temperature-responsive drug release. Macromol Rapid Commun 33, 811-818.
Sun, Q., You, Q., Wang, J., Liu, L., Wang, Y., Song, Y., Cheng, Y., Wang, S., Tan, F., Li, N., 2018. Theranostic nanoplatform: triple-modal imaging-guided synergistic cancer therapy based on liposome-conjugated mesoporous silica nanoparticles. ACS Appl Mater Interfaces 10, 1963-1975.
Suzuki, K., Ikari, K., Imai, H., 2004. Synthesis of silica nanoparticles having a well-ordered mesostructure using a double surfactant system. J Am Chem Soc 126, 462-463.
Tallury, P., Payton, K., Santra, S., 2008. Silica-based multimodal/multifunctional nanoparticles for bioimaging and biosensing applications Nanomedicine 3, 579-592.
Tamanna, T., Bulitta, J.B., Yu, A., 2015. Controlling antibiotic release from mesoporous silica nano drug carriers via self-assembled polyelectrolyte coating. Journal of Materials Science: Mater Med 26, 1-7.
Tang, F., Li, L., Chen, D., 2012. Mesoporous silica nanoparticles: synthesis, biocompatibility and drug delivery. Adv Mater 24, 1504-1534.
Tanwar, J., Das, S., Fatima, Z., Hameed, S., 2014. Multidrug resistance: an emerging crisis. Interdiscip Perspect Infect Dis 2014, 1-7.
Thomas, C.R., Ferris, D.P., Lee, J.-H., Choi, E., Cho, M.H., Kim, E.S., Stoddart, J.F., Shin, J.-S., Cheon, J., Zink, J.I., 2010a. Noninvasive remote-controlled release of drug molecules in vitro using magnetic actuation of mechanized nanoparticles. J Am Chem Soc 132, 10623-10625.
Thomas, M., Slipper, I., Walunj, A., Jain, A., Favretto, M., Kallinteri, P., Douroumis, D., 2010b. Inclusion of poorly soluble drugs in highly ordered mesoporous silica nanoparticles. Int J Pharm 387, 272-277.
Thrall, D.E., Page, R.L., Dewhirst, M.W., Meyer, R.E., Hoopes, P.J., Kornegay, J.N., 1986. Temperature measurements in normal and tumor tissue of dogs undergoing whole body hyperthermia. Cancer R 46, 6229-6235.
Torney, F., Trewyn, B.G., Lin, V.S.-Y., Wang, K., 2007. Mesoporous silica nanoparticles deliver DNA and chemicals into plants. Nat Nanotechnol 2, 295-300.

Torres-Martinez, Z., Delgado, Y., Ferrer-Acosta, Y., Suarez-Arroyo, I.J., Joaquín-Ovalle, F.M., Delinois, L.J., Griebenow, K., 2021. Key genes and drug delivery systems to improve the efficiency of chemotherapy. Cancer Drug Resist 4, 163-191.

pore size of FSM-16 on the entrapment of flurbiprofen in mesoporous structures. Chem pharm bull 53, 974-977.
Trzeciak, K., Chotera-Ouda, A., Bak-Sypien, I.I., Potrzebowski, M.J., 2021. Mesoporous Silica Particles as Drug Delivery Systems—The State of the Art in Loading Methods and the Recent Progress in Analytical Techniques for Monitoring These Processes. Pharmaceutics 13, 1-43.
Vallet-Regí, M., Schüth, F., Lozano, D., Colilla, M., Manzano, M., 2022. Engineering mesoporous silica nanoparticles for drug delivery: where are we after two decades? Chem Soc Rev 6, 1-87.
Vallet-Regí, M., 2012. Mesoporous silica nanoparticles: their projection in nanomedicine. Int Sch Res Notices 2012, 1-20.
Van Rijt, S.H., Bölükbas, D.A., Argyo, C., Wipplinger, K., Naureen, M., Datz, S., Eickelberg, O., Meiners, S., Bein, T., Schmid, O., Stoeger, T., 2016. Applicability of avidin protein coated mesoporous silica nanoparticles as drug carriers in the lung. Nanoscale 8, 8058-8069.
Vega-Villa, K.R., Takemoto, J.K., Yáñez, J.A., Remsberg, C.M., Forrest, M.L., Davies, N.M., 2008. Clinical toxicities of nanocarrier systems. Adv Drug Deliv Rev 60, 929-938.
Wahsner, J., Gale, E.M., Rodríguez-Rodríguez, A., Caravan, P., 2018. Chemistry of MRI contrast agents: current challenges and new frontiers. Chem Rev 119, 957-1057.
Wan, J., Zhang, X., Fu, K., Zhang, X., Shang, L., Su, Z., 2021. Highly fluorescent carbon dots as novel theranostic agents for biomedical applications. Nanoscale 13, 17236-17253.
Wang, K., Yao, H., Meng, Y., Wang, Y., Yan, X., Huang, R., 2015. Specific aptamer-conjugated mesoporous silica–carbon nanoparticles for HER2-targeted chemo-photothermal combined therapy. Acta Biomater 16, 196-205.
Wang, L., Huo, M., Chen, Y., Shi, J., 2017. Coordination-Accelerated "Iron Extraction" Enables Fast Biodegradation of Mesoporous Silica-Based Hollow Nanoparticles. Adv Healthcare Mater 6, 1700720.
Wang, X., Cai, X., Hu, J., Shao, N., Wang, F., Zhang, Q., Xiao, J., Cheng, Y., 2013. Glutathione-triggered "off–on" release of anticancer drugs from dendrimer-encapsulated gold nanoparticles. J Am Chem Soc 135, 9805-9810.
Wang, X., Chen, H., Chen, Y., Ma, M., Zhang, K., Li, F., Zheng, Y., Zeng, D., Wang, Q., Shi, J., 2012. Perfluorohexane-encapsulated mesoporous silica nanocapsules as enhancement agents for highly efficient high intensity focused ultrasound (HIFU). Adv Mater 24, 785-791.
Wang, Y., Han, N., Zhao, Q., Bai, L., Li, J., Jiang, T., Wang, S., 2015. Redox-responsive mesoporous silica as carriers for controlled drug delivery: a comparative study based on silica and PEG gatekeepers. Eur J Pharm Sci 72, 12-20.
Watermann, A., Brieger, J., 2017. Mesoporous silica nanoparticles as drug delivery vehicles in cancer. Nanomaterials 7, 1-17.
Wei, Q., Chen, Y., Ma, X., Ji, J., Qiao, Y., Zhou, B., Ma, F., Ling, D., Zhang, H., Tian, M., 2018. High-Efficient Clearable Nanoparticles for Multi-Modal Imaging and Image-Guided Cancer Therapy. Adv Funct Mater 28, 1704634.
Williams, D.F., 2009. On the nature of biomaterials. Biomaterials 30, 5897-5909.
Wu, L., Wu, M., Zeng, Y., Zhang, D., Zheng, A., Liu, X., Liu, J., 2014. Multifunctional PEG modified DOX loaded mesoporous silica nanoparticle@ CuS nanohybrids as photo-thermal agent and thermal-triggered drug release vehicle for hepatocellular carcinoma treatment. Nanotechnology 26, 025102.
Wu, M., Zhang, H., Tie, C., Yan, C., Deng, Z., Wan, Q., Liu, X., Yan, F., Zheng, H., 2018. MR imaging tracking of inflammation-activatable engineered neutrophils for targeted therapy of surgically treated glioma. Nat Commun 9, 1-13.

Wu, S.-H., Hung, Y., Mou, C.-Y., 2011. Mesoporous silica nanoparticles as nanocarriers. Chem Commun 47, 9972-9985.
Xiao, D., Jia, H.Z., Zhang, J., Liu, C.W., Zhuo, R.X., Zhang, X.Z., 2014. A dual-responsive mesoporous
Xie, M., Shi, H., Ma, K., Shen, H., Li, B., Shen, S., Wang, X., Jin, Y., science, i., 2013. Hybrid nanoparticles for drug delivery and bioimaging: mesoporous silica nanoparticles functionalized with carboxyl groups and a near-infrared fluorescent dye. J Colloid Interface Sci 395, 306-314.
Xue, S., Wang, Y., Wang, M., Zhang, L., Du, X., Gu, H., Zhang, C., 2014. Iodinated oil-loaded, fluorescent mesoporous silica-coated iron oxide nanoparticles for magnetic resonance imaging/computed tomography/fluorescence trimodal imaging. Int Nanomedicine 9, 2527-2538.
Yamauchi, T., Saitoh, T., Shirai, K., Fujiki, K., Tsubokawa, N., 2010. Immobilization of capsaicin onto silica nanoparticle surface and stimulus properties of the capsaicin-immobilized silica. Journal of Polymer Science Part A: Polym Chem 48, 1800-1805.
Yanagisawa, T., Shimizu, T., Kuroda, K., Kato, C., 1990. The preparation of alkyltriinethylaininonium–kaneinite complexes and their conversion to microporous materials. Bull Chem Soc Jpn 63, 988-992.
Yang, H., Chen, Y., Chen, Z., Geng, Y., Xie, X., Shen, X., Li, T., Li, S., Wu, C., Liu, Y., 2017. Chemo-photodynamic combined gene therapy and dual-modal cancer imaging achieved by pH-responsive alginate/chitosan multilayer-modified magnetic mesoporous silica nanocomposites. Biomater Sci 5, 1001-1013.
Yang, H., Li, Y., Li, T., Xu, M., Chen, Y., Wu, C., Dang, X., Liu, Y., 2014a. Multifunctional core/shell nanoparticles cross-linked polyetherimide-folic acid as efficient Notch-1 siRNA carrier for targeted killing of breast cancer. Sci Rep 4, 1-10.
Yang, K.-N., Zhang, C.-Q., Wang, W., Wang, P.C., Zhou, J.-P., Liang, X.-J., 2014b. pH-responsive mesoporous silica nanoparticles employed in controlled drug delivery systems for cancer treatment. Cancer Biol Med 11, 34-43.
Yang, X., He, D., He, X., Wang, K., Zou, Z., Li, X., Shi, H., Luo, J., Yang, X., 2015. Glutathione-Mediated Degradation of Surface-Capped MnO2 for Drug Release from Mesoporous Silica Nanoparticles to Cancer Cells. Part Part Syst Charact 32, 205-212.
Yano, K., Fukushima, Y., 2004. Synthesis of mono-dispersed mesoporous silica spheres with highly ordered hexagonal regularity using conventional alkyltrimethylammonium halide as a surfactant. J Mater Chem 14, 1579-1584.
Yao, Y., Zhou, Y., Liu, L., Xu, Y., Chen, Q., Wang, Y., Wu, S., Deng, Y., Zhang, J., Shao, A., 2020. Nanoparticle-based drug delivery in cancer therapy and its role in overcoming drug resistance. Front Mol Biosci 7, 1-14.
Yoon, S.B., Kim, J.Y., Kooli, F., Lee, C.W., Yu, J.-S., 2003. Synthetic control of ordered and disordered arrays of carbon nanofibers from SBA-15 silica templates. Chem Commun, 1740-1741.
Yu, E., Lo, A., Jiang, L., Petkus, B., Ercan, N.I., Stroeve, P., 2017. Improved controlled release of protein from expanded-pore mesoporous silica nanoparticles modified with co-functionalized poly (n-isopropylacrylamide) and poly (ethylene glycol)(PNIPAM-PEG). Colloids Surf B 149, 297-300.
Yu, F., Wu, H., Tang, Y., Xu, Y., Qian, X., Zhu, W., 2018a. Temperature-sensitive copolymer-coated fluorescent mesoporous silica nanoparticles as a reactive oxygen species activated drug delivery system. Int J Pharm 536, 11-20.
Yu, L., Chen, Y., Wu, M., Cai, X., Yao, H., Zhang, L., Chen, H., Shi, J., 2016. "Manganese extraction" strategy enables tumor-sensitive biodegradability and theranostics of nanoparticles. J Am Chem Soc 138, 9881-9894.
Yu, Z., Zhou, P., Pan, W., Li, N., Tang, B., 2018b. A biomimetic nanoreactor for synergistic chemiexcited photodynamic therapy and starvation therapy against tumor metastasis. Nat Commun 9, 1-9.

Yuan, D., Ellis, C.M., Davis, J.J., 2020. Mesoporous Silica Nanoparticles in Bioimaging. Materials 13, 3795.
Zhang, B., Luo, Z., Liu, J., Ding, X., Li, J., Cai, K., 2014. Cytochrome c end-capped mesoporous silica
vitro and in vivo. J Control Release 192, 192-201.
Zhang, L., Li, Y., Jin, Z., Jimmy, C.Y., Chan, K.M., 2015a. An NIR-triggered and thermally responsive drug delivery platform through DNA/copper sulfide gates. Nanoscale 7, 12614-12624.
Zhang, Q., Liu, F., Nguyen, K.T., Ma, X., Wang, X., Xing, B., Zhao, Y., 2012. Multifunctional mesoporous silica nanoparticles for cancer-targeted and controlled drug delivery. Adv Funct Mater 22, 5144-5156.
Zhang, Z., Liu, C., Bai, J., Wu, C., Xiao, Y., Li, Y., Zheng, J., Yang, R., Tan, W., 2015b. Silver nanoparticle gated, mesoporous silica coated gold nanorods (AuNR@ MS@ AgNPs): low premature release and multifunctional cancer theranostic platform. ACS Appl Mater Interfaces 7, 6211-6219.
Zhao, Q., Geng, H., Wang, Y., Gao, Y., Huang, J., Wang, Y., Zhang, J., Wang, S., 2014a. Hyaluronic acid oligosaccharide modified redox-responsive mesoporous silica nanoparticles for targeted drug delivery. ACS Appl Mater Interfaces 6, 20290-20299.
Zhao, S., Sun, S., Jiang, K., Wang, Y., Liu, Y., Wu, S., Li, Z., Shu, Q., Lin, H., 2019. In Situ Synthesis of Fluorescent Mesoporous Silica–Carbon Dot Nanohybrids Featuring Folate Receptor-Overexpressing Cancer Cell Targeting and Drug Delivery. Nano-Micro Lett 11, 1-13.
Zhao, Z., Huang, Y., Shi, S., Tang, S., Li, D., Chen, X., 2014b. Cancer therapy improvement with mesoporous silica nanoparticles combining photodynamic and photothermal therapy. Nanotechnology 25, 285701.
Zheng, H., Wang, Y., Che, S., 2011. Coordination bonding-based mesoporous silica for pH-responsive anticancer drug doxorubicin delivery. J Phys Chem C 115, 16803-16813.
Zhu, C.-L., Song, X.-Y., Zhou, W.-H., Yang, H.-H., Wen, Y.-H., Wang, X.-R., 2009. An efficient cell-targeting and intracellular controlled-release drug delivery system based on MSN-PEM-aptamer conjugates. J Mater Chem 19, 7765-7770.
Zhu, Y., Fang, Y., Kaskel, S., 2010. Folate-conjugated Fe3O4@ SiO2 hollow mesoporous spheres for targeted anticancer drug delivery. J Phys Chem C 114, 16382-16388.
Zintchenko, A., Ogris, M., Wagner, E., 2006. Temperature dependent gene expression induced by PNIPAM-based copolymers: potential of hyperthermia in gene transfer. Bioconjugate Chem 17, 766-772.
Živojević, K., Mladenović, M., Djisalov, M., Mundzic, M., Ruiz-Hernandez, E., Gadjanski, I., Knežević, N., 2021. Advanced mesoporous silica nanocarriers in cancer theranostics and gene editing applications. J Control Release 337, 193-211.
Zou, Z., He, X., He, D., Wang, K., Qing, Z., Yang, X., Wen, L., Xiong, J., Li, L., Cai, L., 2015. Programmed packaging of mesoporous silica nanocarriers for matrix metalloprotease 2-triggered tumor targeting and release. Biomaterials 58, 35-45.

1771 Table 1. Summary of MSN-based materials-related patents for cancer therapy.

				Type of cell line		
US20160008283A1	2016	Nel et al	Gemcytabine	Pancreatic cancer	MSNs was covered by lipid bilayer which indicate a high loading capacity for anticancer agents	(Nel et al., 2016)
US20140079774A1	2014	Brinker et al	Anticancer agent	Liver cancer	Porous NP-maintained lipid bilayers for targeted delivery	(Brinker et al., 2017)
US8926994B2	2015	Serda et al	TGF-β inhibitor LY364947	Breast cancer	Mesoporous silicon for the production of tumor antigens and adjuvant for anticancer immunity	(Serda et al., 2015)

1772
1773
1774
1775
1776
1777
1778
1779
1780
1781
1782
1783
1784
1785
1786

1787 Table 2. Examples of different stimuli-responsive SMNs.

Stimuli	Type cancer	Type of	Surface	Types of	Size of		Ref.
Magnetic	Breast	MCF-7	Poly (ethyleneimine ne)-b-poly (Nisopropylacrylami de)	Fluorescein and Soybean Trypsin Inhibitor type II−S (STI).	200 nm	Control release of proteins and small molecules in reply to an alternating magnetic field	(Baeza et al., 2012)
	Breast	L929, MCF-7	Fe_3O_4, folic acid	Doxorubicin	750 nm	Attaining a target drug accumulation in tumor tissue, optimum release profile and coexisting diagnostic imaging with therapy based on radial mesoporous silica	(Gao et al., 2018)
	Breast	(MDA-MB-231	Zinc-doped iron oxide, pseudo-rotaxanes	Doxorubicin	-	Display hyperthermic properties when located in an oscillating magnetic field, externally controlled DDS with cancer-killing properties	(Thomas et al., 2010a)
	Breast	MCF-7	Functional inorganic (Au, Fe_3O_4, SiO_2, et) nanocrystals as cores, Gd-Si-DTPA grafted Au@mSiO, Au@SiO2@$mSiO_2$	Doxorubicin	-	Platform for Simultaneous Cell Anticancer Drug Delivery and Imaging	(Chen et al., 2010)
Redox	Brain cancer	U87 MG cells	RGD sequence-enclosing peptide attached through disulfide bonds	Doxorubicin	100 nm	Murder the cancer cell because of the disulfide bonds cleavage through intracellular GSH	(Li et al., 2015b)
	-	HeLa cells	β-CD joined via disulfide bonds	Doxorubicin	200 nm	Simplify the drugs accumulation in cancer environment , longer blood retention half-life, and improve cellular uptake	(de Oliveira Freitas et al., 2017)
	Liver cancer	HepG2 cells	MnO_2 nanostructure	Doxorubicin	120 nm	GSH-responsive DDS will causing a novel production of nanodevices for intracellular controlled delivery	(Yang et al., 2015)
Light	-	Hep-G2	Pd@Ag nanoplates as core	Doxorubicin	150 nm	Chemotherapy and PTT and for killing tumor cells.	(Fang et al., 2012)
	-	MCF-7 Hela	Pure coumarin derivative or anticancer drug chlorambucil functionalized with 7-amino-coumarin derivative was attached onto the AP-MSN surface	Chlorambucil	130 nm	Irradiation of either one- or two photons excitations induced controlled release of anticancer drug, good biocompatibility, cellar uptake property, and efficient photo regulated drug release	(Lin et al., 2010)

	Pancrea tic and	PANC-1 and SW480	incorporate 4-phenylazoaniline (4-PAA) into the particle pores	Camptothecin		Light-activated nanoimpeller-controlled drug release in cancer	(Lu et al., 2008)
Enzyme	Breast cancer	MDA-MB-231 cell	Poly (â-amino esters)	Doxorubicin	-	Releases DOX in acidic solution or in the existence of porcine liver esterase	(Deniz áYilmaz and Fraserá Stoddart, 2015)
	Breast cancer	HeLa	Rotaxane, azido-GFLGR7RGDS, sev en arginine	Doxorubicin	130 nm	Progress avoidance to αv-β3-positive HeLa cancer cells	(Cheng et al., 2015)
	Liver cancer	HepG2 tumor bearing	Serum albumin attached through polypeptide linker	Doxorubicin	200 nm	Anticancer drug loading capacity could proficiently cause cell apoptosis *in vitro* and avoid tumor growth with least side effects.	(Liu et al., 2015a)
Temperature	Breast cancer	MCF-7 cells	DNA marked copper sulfide nanospheres	Doxorubicin	~140-200 nm.	NIR-responsive and temperature DOX release, with an enhanced release rate with GSH behavior and used as anticancer drug delivery carrier with triggered drug release and effective anticancer behavior *in vitro* subsequently NIR irradiation.	(Zhang et al., 2015a)
	Cervical cancer	HeLa cells	Poly(2-(dimethylamino) ethyl methacrylate)	Doxorubicin	-	Biocompatible MSNs-coated zwitterionic sulfobetaine copolymer for temperature-responsive release of drug	(Sun et al., 2012)
pH	Bladder cancer	T 24 cells	Poly (2-vinyl pyridine)	Doxorubicin	90 nm	Indicating pH-triggered release in the endosome, light-triggered endosomal escape with an on-board photosensitizer, and effective folic acid-based cell targeting.	(Niedermayer et al., 2015)
	Cervical cancer	HeLa	Alginate/chitosan polymer	Doxorubicin	167.4 nm	Safe and operative drug-delivery systems with good tissue compatibility.	(Feng et al., 2014)
Ultrasound	-	L929	Dibenzo-crown ethers	Doxorubicin	200 nm	Superparamagnetic iron oxide core with core@shell NPs, shell of mesoporous silica, and crown ether boundary was prepared for tumor cell imaging and drug delivery	(Lee et al., 2013)

1788

1789 Table 3. Summary of applications of MSN-based materials for cancer treatment.

MSN	Material	Surface	Cell type	Cancer	Applications	Ref
Magnetic MSNs	VEGF shRNA and DOX	PEI, folic acid	HeLa cell	-	The targeting co-delivery of chemotherapeutic agents and nucleic acid drugs	(Li et al., 2016)
HMSNs	photosensitizer chlorin e6 (Ce6), GOx, bis[2,4,5-trichloro-6-(pentyloxycarbonyl)phenyl] oxalate (CPPO), perfluoro hexane (PFC)	$-NH_2$ Cancer cell coating	B16-F10	Lung	Synergistic chemical photodynamic-starvation treatment to inhibit tumor metastasis.	(Yu et al., 2018b)
	GSH	-	MCF-7	Breast	Glutathione-sensitive hollow MSNs showed a high loading amounts of DOX, due to the large voids that might exist in the structures.	(Moghaddam et al., 2018)
MSNs	VEGF	SiRNA, PEI capping, PEGylation and fusogenic peptide KALA modification	A549 cells, L02 cells, PC-3 and HCCLM-3	Lung	Reduction of lung cancer growth and metastasis	(Chen et al., 2014c)
MSNs	DOX	Sub-6 nm CuS nanodots coating	Sub-q MDA-MB-231 cells HepG2 cells	Liver	Photoacoustic (PA) and infrared (IR) thermal imaging-guided synergistic cancer treatment	(Wei et al., 2018)
MSNs	Gemcitabine (GEM), Paclitaxel (PTX)	lipid bilayer	xenograft and orthotopic animal models,	Pancreatic	Pancreatic cancer therapy	(Meng et al., 2015)
MSNs	PEGylated lipid bilayer covering	Axitinib Celastrol	Sub-q SCC7 cells	Breast	Effective delivery of drug to the cancer site with improved effects on angiogenesis and	(Choi et al., 2016)

					mitochondrial function, avoid of cell proliferation apoptosis, anti-angiogenesis, improved antitumor function.	
Magnetic mesoporous silica nanocomposites	Dox, Ce6	Alginate/chitosan	Breast cancer cell line (MCF-7)	-	Dual-modal cancer imaging and synergistic chemo-photodynamic with gene therapy	(Yang et al., 2017)
MSNs	PEG/PDA, AS-1411 aptamer enveloping	CX-5461	Sub-q HeLa cells	Cervical	Cancer treatment via induction of selective pro-death autophagy	(Duo et al., 2018)
Hollow mesoporous spheres	DOX	folate-conjugated rattle-type Fe_3O_4@SiO_2	Hela cells	-	Synergistic targeted anticancer with receptor-mediated and magnetic targeting	(Zhu et al., 2010)
HMSNs	DOX	Au nanostar, RGD coating	Sub-q U87MG cells	Brain	Targeted photothermal and chemotherapy of cancer cells	(Li et al., 2017a)
MSNs	DOX	Transferinin	Human pancreatic cancer cells, MiaPaCa-2	Pancreatic	Multifunctional MSN delivery system include pH-sensitive nanovalves fluorescent molecules, and targeting proteins to improve the treatment of cancer	(Hwang et al., 2015)
MSNs	PLH and PEG covering	Sorafenib	Sub-q H22 cells	-	pH-controlled system can be triggered to drug release in tumor specific	(Mu et al., 2017)
MSNs	CPT or paclitaxel (TXL)	phosphonate and folic acid	PANC-1 and BxPC3 cells	pancreatic cancer	Magnetic resonance and fluorescence imaging, drug delivery, cell Targeting, and magnetic manipulation	(Liong et al., 2008)
Gd-doped MSNs	ICG-loaded thermosensitive	DOX	Sub-q 4T1 cells	Breast	Triple-modal imaging-guided synergistic	(Sun et al., 2018)

	liposomes				treatment of tumor	
MSNs	Camptothecin	and galactose	(HCT-116), (Capan-1) and 231)	Colorectal breast	Photodynamic therapy and drug	(Zhao et al.
Mesoporous silica bounded gold nanorod	Attached with b-cyclodextrin Peptide RLA ([RLARLAR] 2) Polymer CS(DMA)-PEG	ICG	Sub-q MCF-7 cells	-	PDT with PTT is a combination therapy for extension of tumor-bearing mice survival time	(Williams, 2009)
MSNs	DOX	TAT peptide	Hela cells	-	Cell-nuclear targeted DDS	(Pan et al., 2012)
Magnetic MSNs	DOX	Neutrophils carrying	Intracranially injection C6-Luc or U87-Luc	Brain tumor	MR imaging tracking of inflammation-activatable engineered neutrophils for targeted therapy	(Wu et al., 2018)
Magnetic silica	doxorubicin and paclitaxel	Transferrin, PLGA	glioma cells, U-87 and bEND.3	Brain cancer	The low penetration across the blood-tumor barrier (BTB) and malignant brain glioma across the blood brain barrier (BBB)	(Cui et al., 2013)
MSNs	Camptothecin	Folic acid, PEI	Panc-1	Breast	Introduction of fluorescent and targeting moieties	(Rosenholm et al., 2009)
MSNs	MTX	Methotrexate	HeLa	-	Specific induction of apoptosis, targeted delivery of the chemotherapeutic	(Rosenholm et al., 2010)
silica nanospheres	Bovine serum albumin (BSA)	Hollow chitosan	MCF-7	Breast	pH-sensitive targeted delivery	(Deng et al., 2011)
MSNs	DOX	RGDFFFFC	U-87 MG, COS7	-	pH- and redox-dual-responsive tumor-triggered targeting	(Xiao et al., 2014)
MSNs	DOX	Sgc8	Hela	Breast Cancer	Spatio-temporal control to cancer therapy	(Xiao et al., 2014)
MSNs	Camptothecin	Hyaluronic acid	MCF-7, L929	-	Targeting specific tumor cells over-expressing the CD44 protein	(Ma et al., 2012)
MSNs	TPE-PDT	Mannose	MDA-MB-231 ,MCF-7 ,HCT-116	Breast	photodynamic therapy in cancer treatment	(Ma et al., 2012)

MSNs	Sunitinib	cRGDyK	U87MG	-	PET image-guided DDS and tumor vasculature	(Chakravarty et al., 2015)
Fluorescent MSNs	Camptothecin	trihydroxysilylpropyl methylphosphonate	Capan-1, AsPc-1, and PANC-1	Pancreatic, colon, stomach	Minimum leakage of drug into the buffer solution and cell medium, delivery system of hydrophobic anticancer drugs	(Lu et al., 2007)

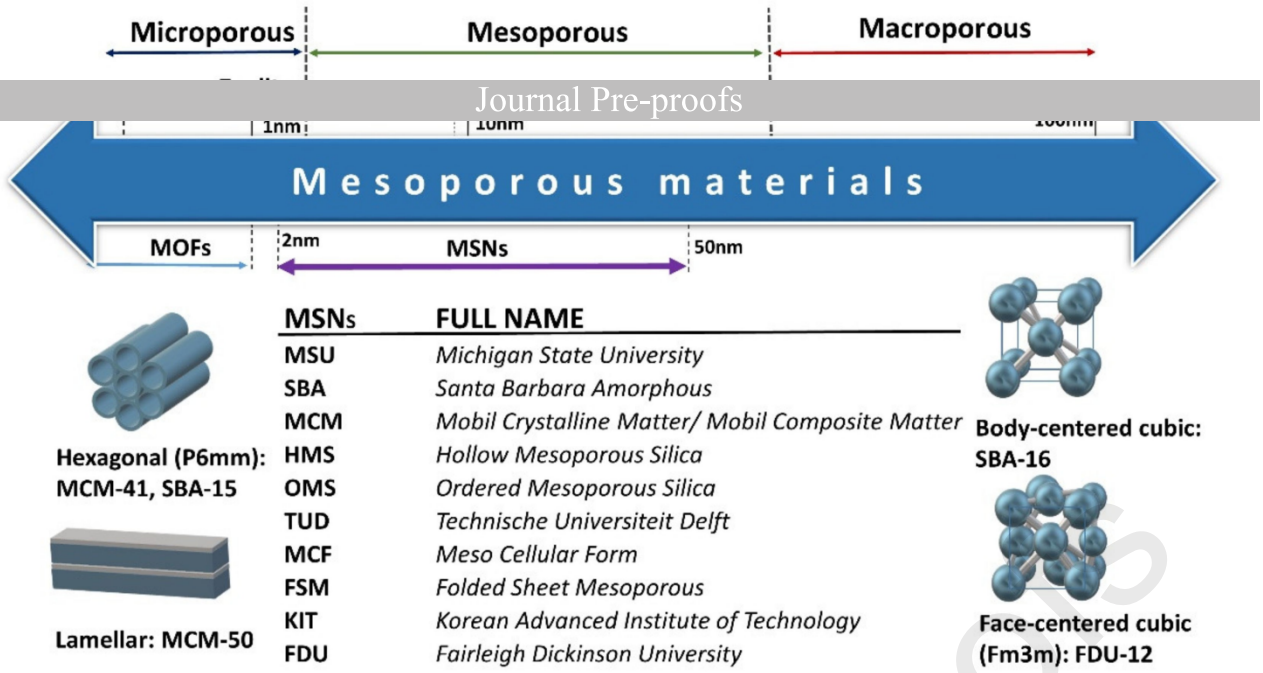

Figure 1. Schematic depiction of various mesoporous materials utilized as DDSs (Trzeciak et al., 2021).

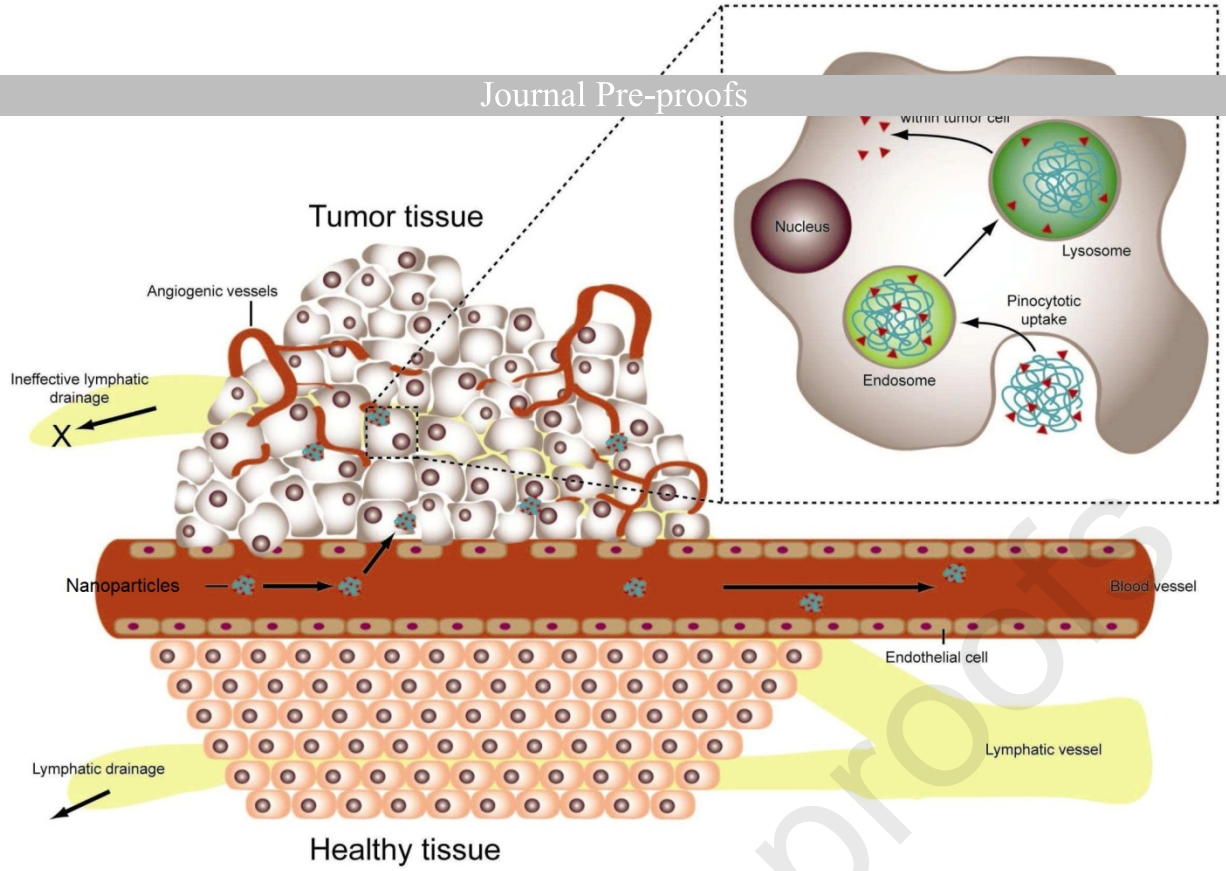

Figure 2. Schematic depiction of the EPR effect: passive targeting to tumor tissue is achieved by extravasation of NPs through the increased permeability of the tumor vasculature and ineffective lymphatic drainage (Fox et al., 2009).

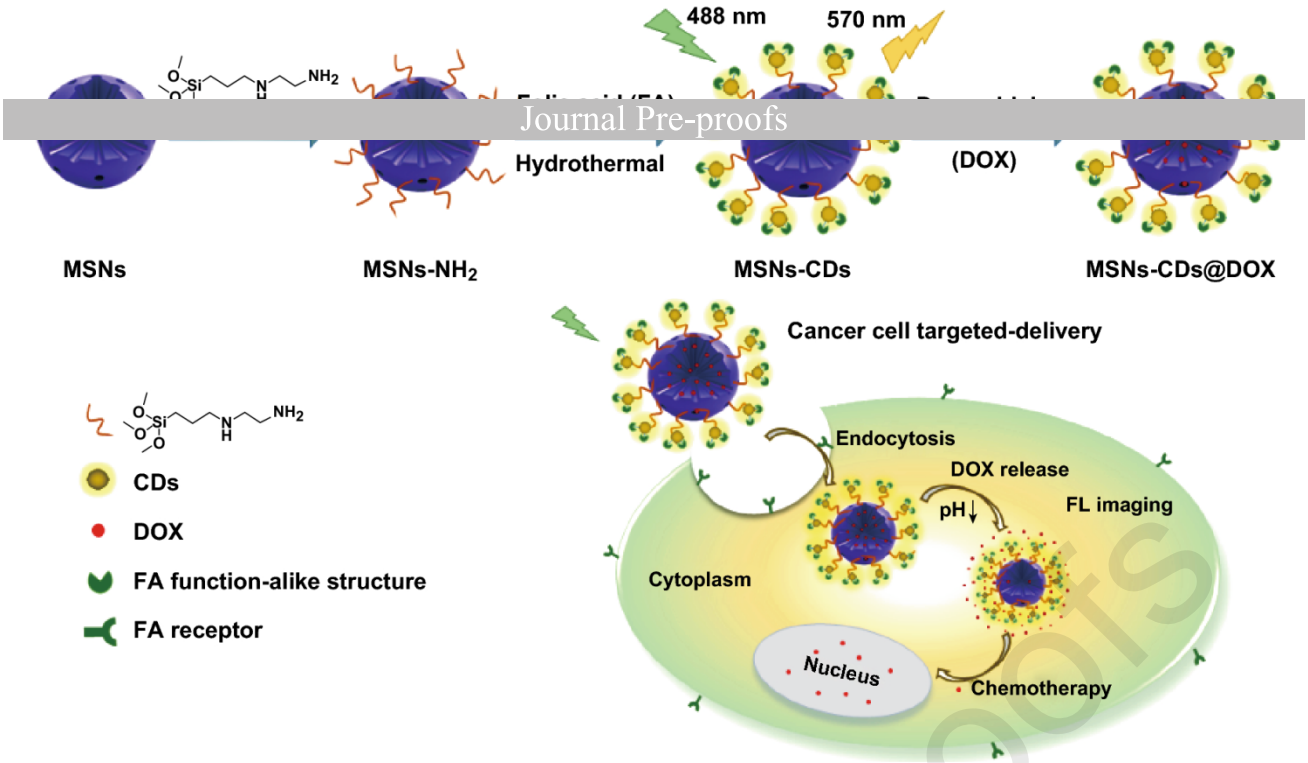

1807
1808 Figure 3. Schematic representation of the preparation process and fluorescence imaging-guided
1809 antitumoral drug delivery application of MSNs-CDs nanohybrid (Zhao et al., 2019).

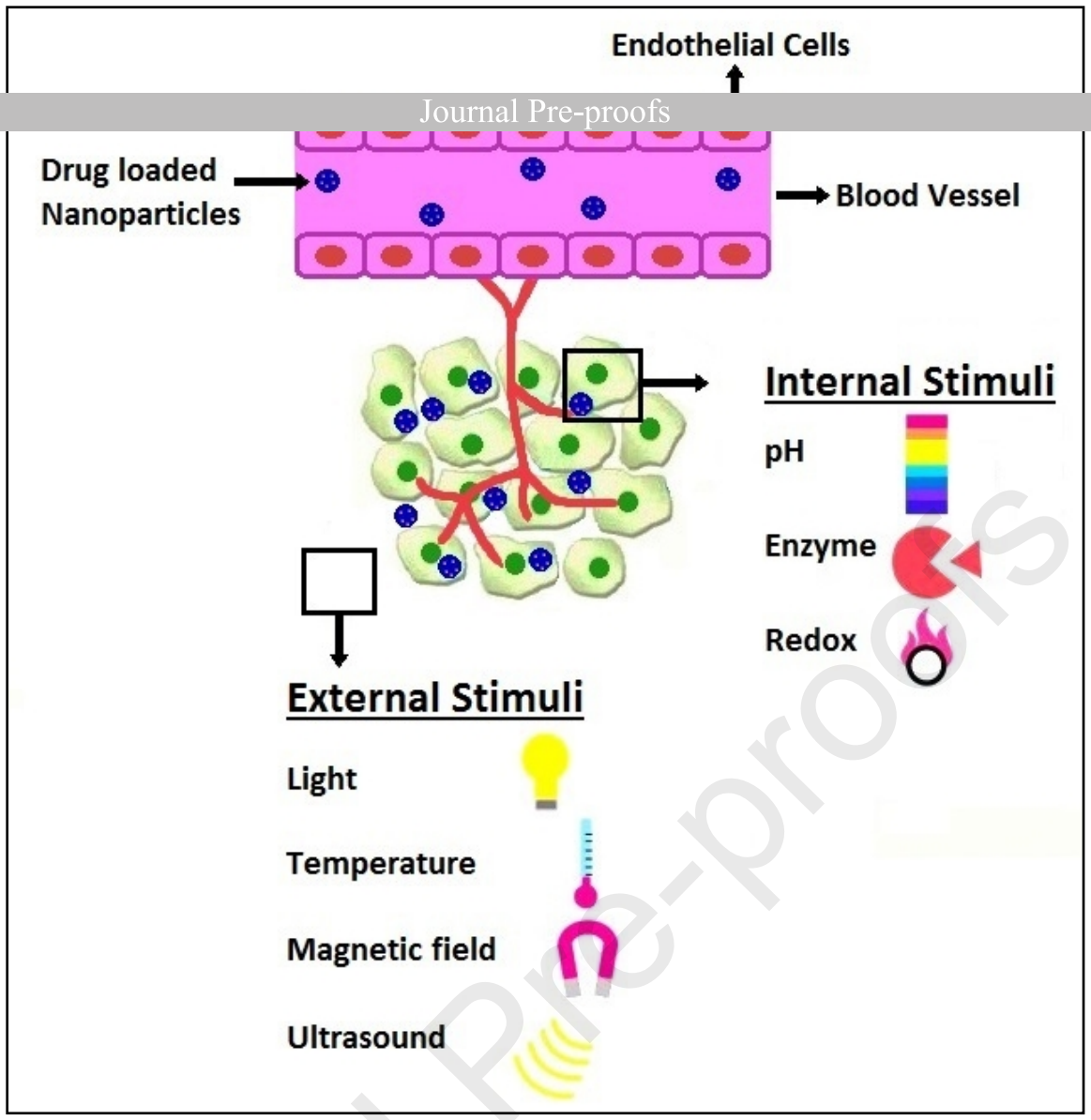

1810

1811 Figure 4. Schematic representation of the various stimuli applied for the controlled release of

1812 chemotherapeutics (Kang et al., 2018).

1813

1814

1815

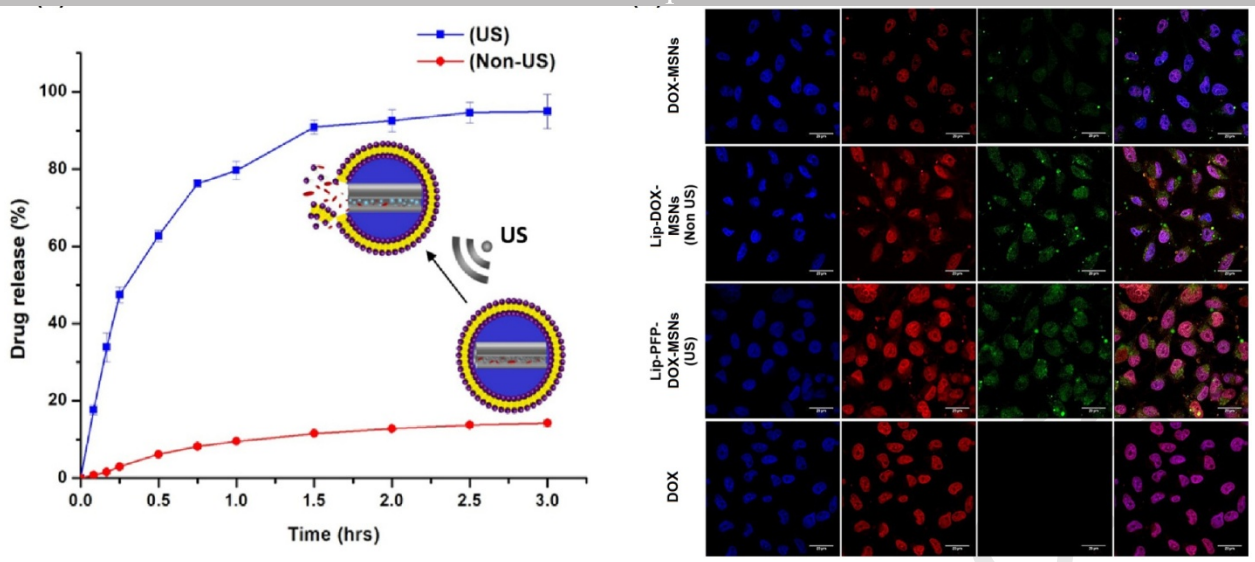

Figure 5. (**A**) *In vitro* release profile of DOX from Lip-PFP-DOX-MSNs and Lip DOX-MSNs with and without US-irradiation. (**B**) Cellular uptake studies with confocal microscopy with FITC (green) labelled NPs. DOX-MSNs, Lip-DOX-MSNs (Non-US), and Lip-PFP-DOX-MSNs (US), showing localization of DOX (red) in the nuclei, stained with DAPI (blue). Scale bar is 20 µm (Amin et al., 2021).

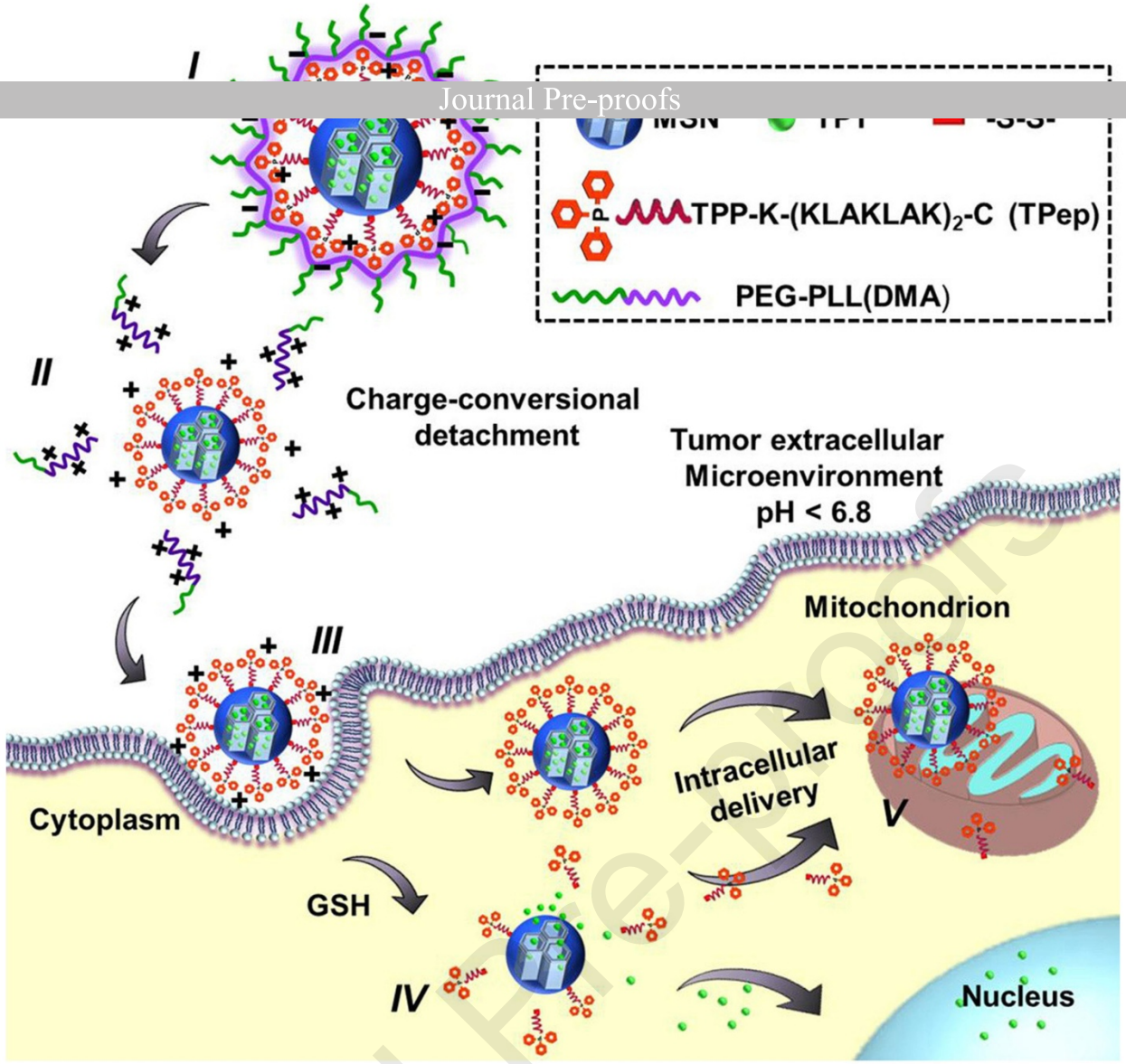

Figure 6. Schematic of the delivery process: (I) multifunctional enveloped nanosystem under neutral pH, (II) detachment of PEG-PLL chains in acidic tumor microenvironment, (III) Electrostatic interaction between cationic NPs and negatively charged cell membrane, (IV) intracellular GSH-triggered TPT and TPep release, (V) specific binding and mitochondria disruption (Luo et al., 2014).

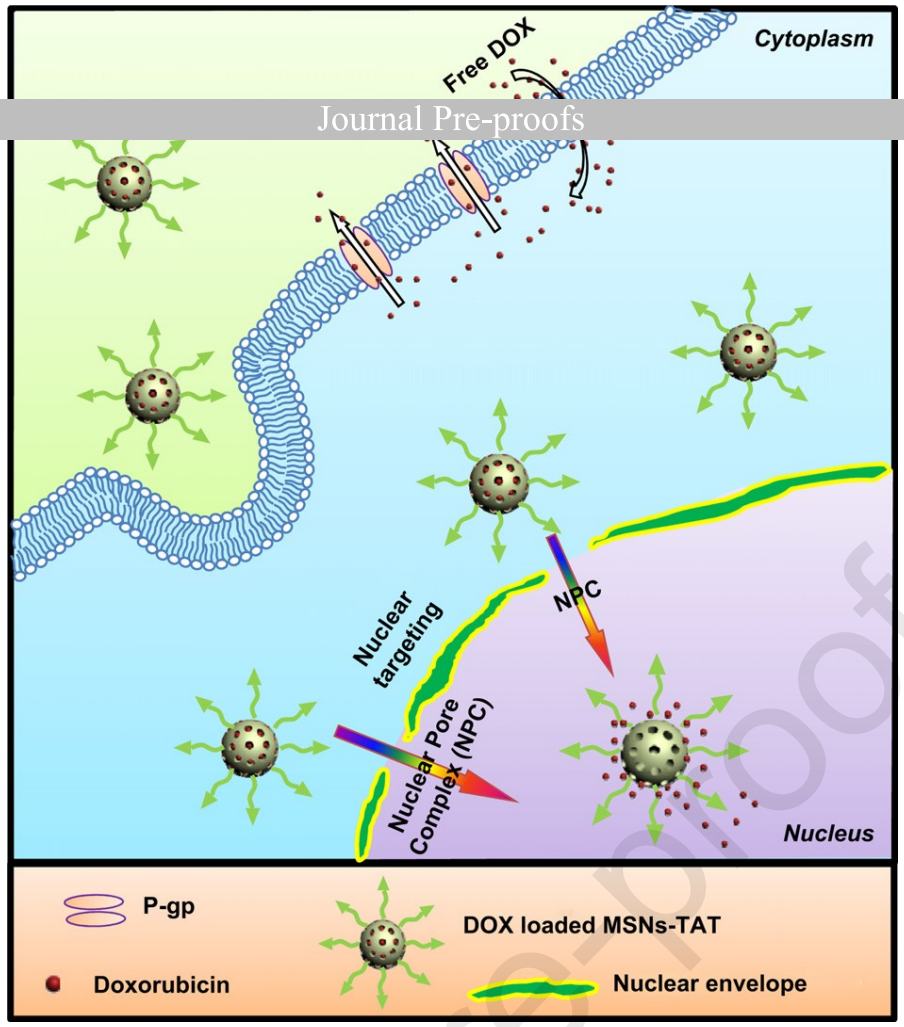

Figure 7. Schematic depiction of nuclear-targeted DDS based on MSNs modified with TAT peptide to overcome MDR with enhanced chemotherapy efficacy (Pan et al., 2013).

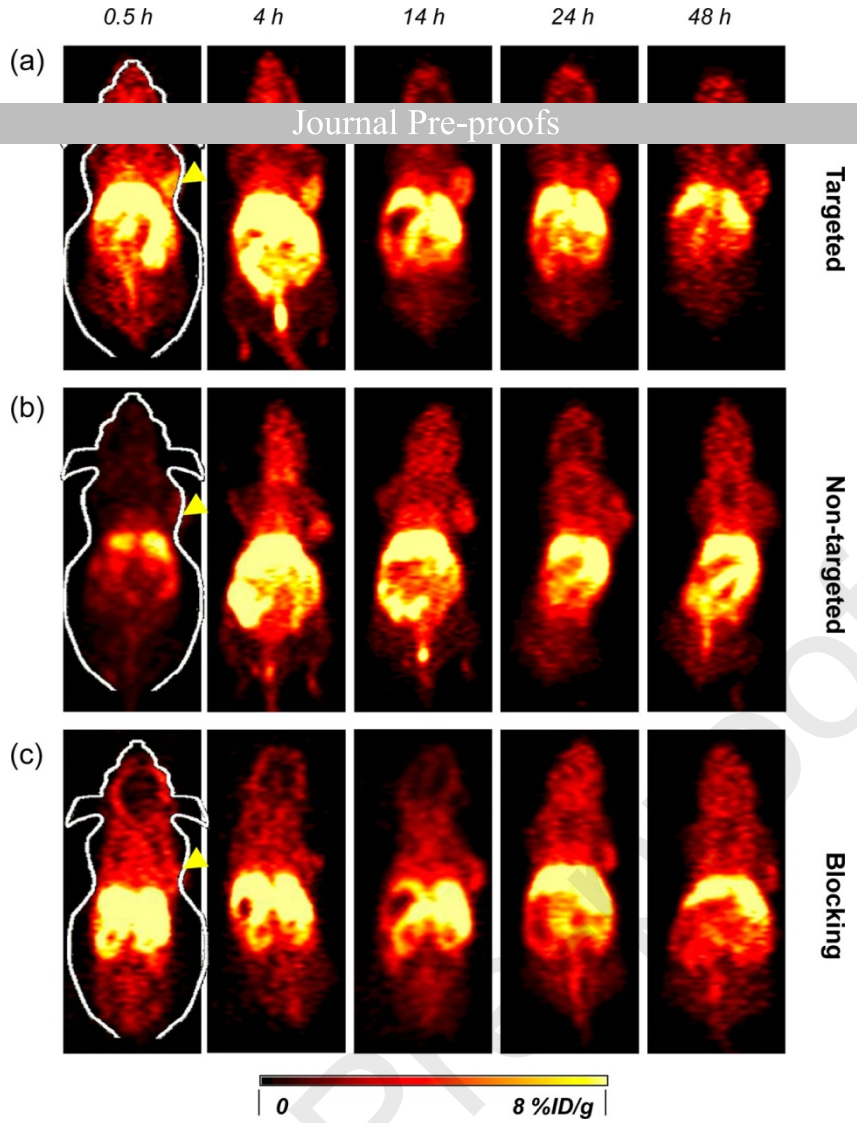

1833

1834 Figure 8. PET images of 4T1 tumor-bearing mice at different time points post-injection of (a)
1835 Cu-MSN-800CW-TRC105(Fab), (b) Cu-MSN-800CW, and (c) Cu-MSN-800CW-TRC105(Fab)
1836 with a blocking dose of TRC105 (1 mg/mouse). The yellow arrowheads display tumors (Chen et
1837 al., 2014b).

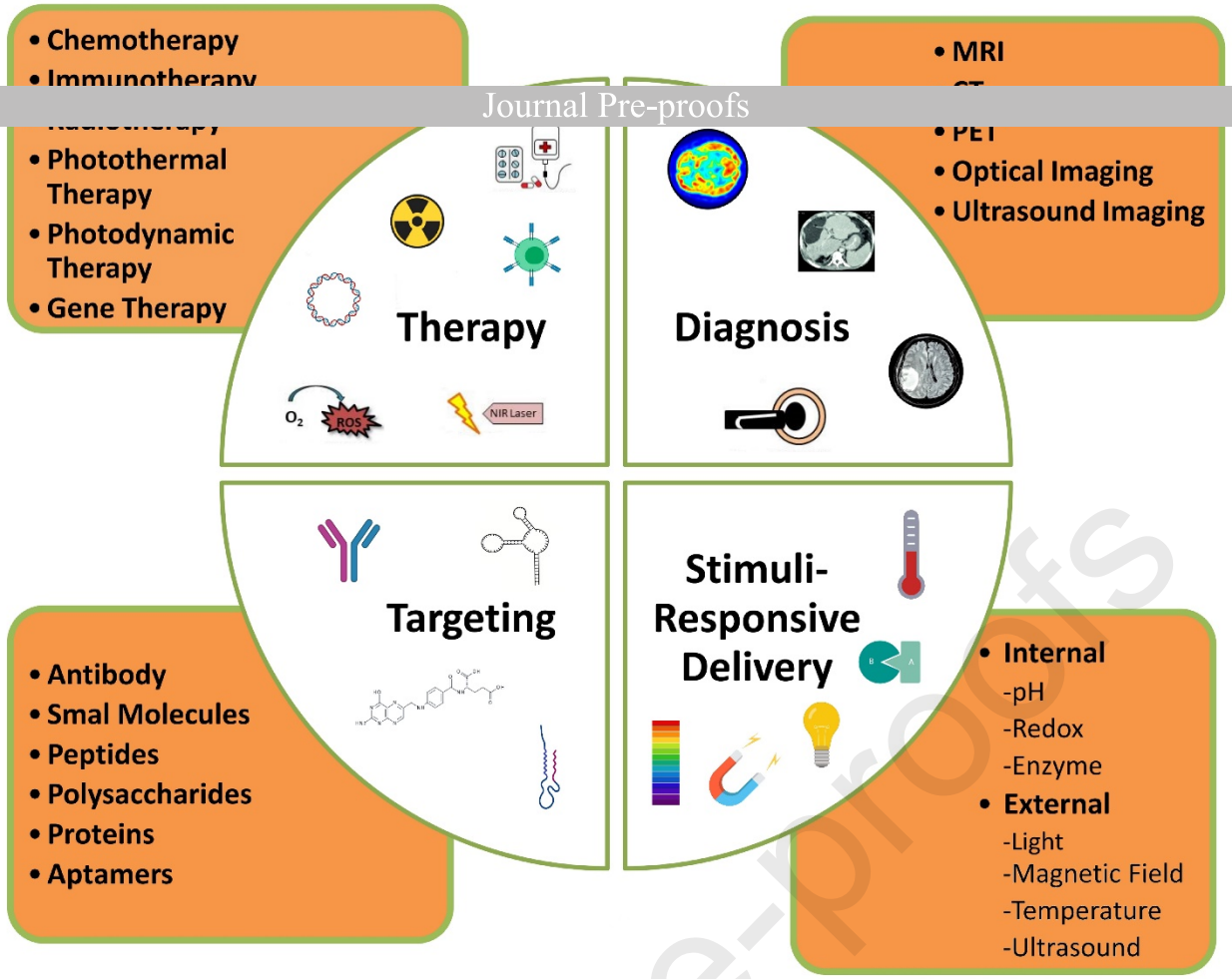

Authors contribution: Fatemeh Ahmadi, Arezoo Sodagar Taleghani, Pedram Ebrahimnejad: Wrote and revised the manuscript. Seyyed Pouya Hadipour Moghaddam, Farzam Ebrahimnejad: Co-wrote the manuscript. Kofi Asare-Addo: reviewed and edited the manuscript. Ali Nokhodchi: revised the manuscript and supervised the research.

Declaration of interests

☒ The authors declare that they have no known competing financial interests or personal relationships that could have appeared to influence the work reported in this paper.

☐The authors declare the following financial interests/personal relationships which may be considered